THE EFFECTS OF STRUCTURAL MODIFICATIONS ON ACOUSTIC CHARACTERISTICS OF ENCLOSED BODIES

A THESIS SUBMITTED TO
THE GRADUAL SCHOOL OF NATURAL AND APPLIED SCIENCES
OF
MIDDLE EAST TECHNICAL UNIVERSITY

BY

ÖZLEM DEMİRKAN

IN PARTIAL FULLFILLMENT OF THE REQUIREMENTS
FOR
THE DEGREE OF MASTER OF SCIENCE
IN
MECHANICAL ENGİNEERING

JULY 2010

Approval of the thesis:

THE EFFECTS OF STRUCTURAL MODIFICATIONS ON ACOUSTIC CHARACTERISTICS OF ENCLOSED BODIES

submitted by **ÖZLEM DEMİRKAN** in partial fulfillment of the requirements for the degree of **Master of Science in Mechanical Engineering Department, Middle East Technical University** by,

Prof. Dr. Canan Özgen _____
Dean, Graduate School of **Natural and Applied Sciences**

Prof. Dr. Suha Oral _____
Head of Department, **Mechanical Engineering**

Prof. Dr. H. Nevzat Özgüven _____
Supervisor, **Mechanical Engineering Dept., METU**

Prof. Dr. Mehmet Çalışkan _____
Co-Supervisor, **Mechanical Engineering Dept., METU**

Examining Committee Members:

Prof. Dr. Y. Samim Ünlüsoy _____
Mechanical Engineering Dept., METU

Prof. Dr. H. Nevzat Özgüven _____
Mechanical Engineering Dept., METU

Prof. Dr. Mehmet Çalışkan _____
Mechanical Engineering Dept., METU

Asst. Prof. Dr. Ender Ciğeroğlu _____
Mechanical Engineering Dept., METU

Asst. Prof. Dr. İpek Başdoğan _____
Mechanical Engineering Dept., KOÇ University

Date: 15.07.2010

I hereby declare that all information in this document has been obtained and presented in accordance with academic rules and ethical conduct. I also declare that, as required by these rules and conduct, I have fully cited and referenced all material and results that are not original to this work.

Name, Last name : Özlem DEMİRKAN

Signature :

ABSTRACT

THE EFFECTS OF STRUCTURAL MODIFICATIONS ON ACOUSTIC CHARACTERISTICS OF ENCLOSED BODIES

Demirkan, Özlem
M.S., Department of Mechanical Engineering
Supervisor: Prof. Dr. H. Nevzat Özgüven
Co-Supervisor: Prof. Dr. Mehmet Çalışkan

July 2010, 114 pages

Low frequency noise caused by vibrating panels can pose problems for vehicles from noise, vibration and harshness (NVH) standpoint. In order to reduce interior noise levels in cars, some structural modifications are required on the car body. Structural modifications studied in this work are stiffeners welded on the walls of enclosed structure to change vibration characteristics. In this thesis, interaction between acoustic domain inside closed structures and their vibrating enclosing boundaries are analyzed. Analysis of vibro-acoustic behavior includes frequency response analysis of structure by Finite Element Method (FEM) and sound pressure level (SPL) prediction of the cabin interior by Boundary Element Method (BEM). The standard parts of the analyses are performed using available CAE (Computer Aided Engineering) software.

It is demonstrated that the structural modification technique integrated with the vibro-acoustic model of the system reduces the computational effort considerably. The frequency response functions of a structure for each modification can easily be obtained in a fast and efficient way by using the structural modification technique. Thus, effects of design changes in the structure body on noise levels due to vibration of the structure can be very handily and efficiently studied. In the case studies presented, the effects of various different stiffeners applied on a simple closed structure are studied in detail.

Keywords: Structural Modification, Structural Dynamics, Noise, Vibro-Acoustics.

ÖZ

YAPISAL DEĞİŞİKLİKLERİN
KAPALI HACİMLERİN AKUSTİK ÖZELLİKLERİNE ETKİSİ

Demirkan, Özlem
Yüksek Lisans, Makine Mühendisliği Bölümü
Tez Yöneticisi: Prof. Dr. H. Nevzat Özgüven
Ortak Tez Yöneticisi: Prof. Dr. Mehmet Çalışkan

Temmuz 2010, 114 sayfa

Panellerin titreşiminden kaynaklanan düşük frekanstaki gürültü araçlarda gürültü, titreşim ve konfor açısından sorun yaratabilir. Araçların içindeki ses düzeyinin azaltılması için gövdede bazı yapısal değişiklikler gereklidir. Bu çalışmadaki yapısal değişiklikler aracın titreşim özelliklerini değiştirmek için şasiye kaynakla birleştirilen güçlendirici çubuklardır. Bu tezde, aracın içindeki akustik ortam ile bu ortamı çevreleyen ve titreşen sınırların etkileşimi incelenmiştir. Titreşim akustiği incelemesi, yapının Sonlu Eleman Metoduyla frekans tepki analizini, kabin içinde Sınırlı Elemanlar Metodu ile ses basınç düzeyi kestirimlerini içerir. Çözümlemelerin standart kısımları mevcut Bilgisayar Destekli Analiz yazılımları kullanılarak yapılmıştır.

Titreşim akustiği modeli ile bütünleşik yapısal değişiklik yöntemi hesaplama zahmetini oldukça azaltır. Bir yapının frekans tepki fonksiyonu yapısal değişiklik metodu kullanılarak hızlı ve etkili bir şekilde elde edilebilir.

Buradan hareketle aracın gövdesinde yapılan tasarım değişikliklerinin arabanın içinde yapının titreşiminden kaynaklanan ses düzeyine etkisi üzerine çok basit ve etkili bir şekilde çalışılabileceği gösterilmiştir. Sunulan örnek çalışmalarda, basit kapalı bir yapıya uygulanan çeşitli güçlendirici çubukların etkisi üzerine detaylı olarak çalışılmıştır.

Anahtar Kelimeler: Yapısal Değişiklik, Yapı Dinamiği, Gürültü, Titreşim Akustik Etkileşimi.

To my dear parents and

to my grandmothers Zeynep Demirkan & Hayriye Özdin, in the name of all women in my country who had given no chance for education

with love and gratitude…

ACKNOWLEDGEMENTS

I would like to express my deepest appreciation to Prof. Dr. H. Nevzat Özgüven and Prof. Dr. Mehmet Çalışkan for their excellent supervision, guidance and criticism, which formed the basis of this work.

I would also like to express my sincere gratitude to Asst. Prof. Dr İpek Başdoğan for her invaluable support in this study. The discussions with Assoc. Prof. Altan Kayran are gratefully acknowledged.

I would like to thank my colleges Salih Alan and Güvenç Canbaloğlu for their insightful discussions and supports. Also I would like to thank Gülşen Kamçı and Erdem Yüksel for their help in teaching the LMS Virtual Lab Software. I am also grateful to my dearest friends Tuğçe Yüksel, Bekir Bediz, M. Ersin Yümer, Bilge Koçer, Ulaş Yaman, Onur Taylan and H. Sinem Şaş for their friendship and technical support during the thesis period.

I also would like to express my appreciation to Eray Göksu for his endless support and patience.

Also I would like to express my deepest feelings to my dearest parents, Sevgi Demirkan and Yaseddin Demirkan, for everything they have done to encourage and support me.

The author would like to thank to Scientific and Research Council of Turkey (TÜBİTAK) that supports her through a Fellowship and through the project 108M288.

TABLE OF CONTENTS

LIST OF TABLES

TABLES

LIST OF FIGURES

FIGURES

LIST OF SYMBOLS

a : Length of elastic plate

b_s : Body forces

c : Speed of sound

C : Geometrical coupling matrix

d_n : Vibration displacement in the normal direction

$[D]$: Dynamic stiffness matrix

D_S : Constitutive matrix

E : Modulus of elasticity

$[E]$: Subsystem energies

$\{F\}$: Generalized forcing vector

F_A : Acoustic load vector

F_S : Structural load vector

G : Shear modulus

$G(r, r_s)$: Free space Green's function

h : Thickness of elastic plate

H : Spatial coupling matrix

$[H]$: Structural damping matrix

$H(\omega)$: Indirect BEM influence matrix

i : Unit imaginary number

I : Mass moment of inertia

$[I]$: Identity matrix

k : Wave number

$[K]$: Stiffness matrix

$[L]$: Matrix containing internal and coupling loss factors

L_x, L_y, L_z : Dimensions of enclosed fluid domain in Cartesian coordinates

m : Mass of subsystem

$[M]$: Mass matrix

$[\Delta H]$: Structural damping matrix of modifying structure

$[\Delta K]$: Stiffness matrix of modifying structure

$[\Delta M]$: Mass matrix of modifying structure

n : Normal vector

n_i : Subsystem modal density

n_F : Boundary normal vector in FEM

N_F : Acoustic shape function

N_S : Structural shape function

p : Acoustic pressure

p_0 : Equilibrium pressure of the acoustic medium

$\hat{p}$: Amplitude of harmonic acoustic pressure

P : Total pressure

q : Acoustic source term

r : Point inside the acoustic domain

r_s : Point on the surface of acoustic domain

R : Power transfer coefficient

t : Time

t_s : Surface traction vector

u_n : Structure surface normal velocity

V_F : Volume of acoustic medium

$\{x\}$: Generalized displacement vector

$[\alpha]$: Receptance matrix of original structure

$[\gamma]$: Receptance matrix of modified structure

γ_r : r^{th} mode structural damping ratio

γ_s : Structural damping ratio for all modes

δ : Dirac's delta function

η_i : Subsystem damping loss factor

η_{ij} : Coupling loss factor between subsystems

$\{\eta(\omega)\}$: Modal participation vector of acoustic domain

ϑ_n : Normal velocity of acoustic particles

λ , μ : Lame coefficients

λ_{ij} : Dimensionless frequency parameter

λ_B : Bending wave length of plate

ν : Poisson's ratio

$[\Pi]$: Input power matrix

ρ : Density change

ρ_0 : Equilibrium density of the acoustic fluid

ρ_s : Density of structure material

$\underline{\rho}$: Total density in the acoustic medium

σ : Single layer potential (jump of velocity)

τ : Double layer potential (jump of pressure)

υ_F : Test function used in FEM

υ_s : Outward normal vector of acoustic domain surface in BEM

$\{\phi^r\}$: r^{th} mode shape

$[\phi_n]$: Modal matrix of the acoustic domain

Φ_a : Acoustic wave function

ω : Circular frequency

ω_r : r^{th} natural frequency

$\langle p^2 \rangle$: Space averaged pressure velocities

$\langle v^2 \rangle$: Space averaged vibration velocities

LIST OF ABBREVIATIONS

ATV	: Acoustic transfer vector
BEM	: Boundary element method
ES	: Element size
FE	: Finite element
FEM	: Finite element method
FRAC	: Frequency response assurance criterion
FRF	: Frequency response function
FRSF	: Frequency response scale factor
MATV	: Modal acoustic transfer vector
PACA	: Panel acoustic contribution analysis
SEA	: Statistical energy analysis
SMT	: Structural modification technique
SPL	: Sound pressure level
TPA	: Transfer path analysis
WBM	: Wave based method

CHAPTER 1

INTRODUCTION

1.1 Objective

Sound level prediction at early design stages has become extremely important for car manufacturers since there is a competition to design more comfortable and silent vehicles. Demand on better sound quality is ever growing. This leads designers to diagnose and fix the causes of poor sound quality.

Noise inside a vehicle can be classified as air-borne and structure-borne noise. Air-borne noise is caused when there is not enough sealing between interior and exterior of cabin or when there is sound transmission between the panels of the cabin. Air-borne noise occurs at high frequencies and can be controlled by adding absorbing materials. Vibration of panels due to mechanical excitations causes structure-borne noise which occurs at low frequencies. Engine vibration, tyre road interaction noise and transmission vibration may be the causes of structure-borne noise inside vehicles.

The objective of this thesis is to develop a method to predict effect of structural modifications on the acoustic response at discrete points inside closed spaces having vibrating boundaries. Low frequency structure-borne

noise caused by vibrating panels is considered and vibration response is changed by addition of proper stiffeners to the selected panel. Response function of original structure is obtained by Finite Element Method (FEM). Then, dynamic response after structural modifications is obtained by Özgüven's structural modification method for additional degrees of freedom [1], so the dynamic analysis of modified structure is not repeated after each modification. Vibration displacements or velocities are used as boundary conditions for analyzing the acoustic domain by BEM. Sound pressure at desired points can be found easily after structural modifications without analyzing the modified system from the beginning.

1.2 Literature Survey

A survey of previous work including sound level prediction inside vehicle like structures and structural modification techniques is presented below.

Noise inside cavities can be analyzed by experimental, analytical and numerical methods. It is aimed to save time in the design process of products, so numerical methods are developed to analyze the systems and to find optimum design parameters for quiet and comfortable products. Moreover, geometrical complexities of structures require numerical solution techniques. FEM, BEM and Statistical Energy Analysis (SEA) are the most common techniques used in the acoustic field analysis.

In the literature review by Lalor and Priebsch [2], numerical methods to solve vibro-acoustic problems were presented. The causes of noise inside vehicles and noise characteristics were discussed.

Kim et al. [3] studied interior sound pressure field of a vehicle by FEM. Interior acoustic pressure was formulated explicitly by using structural and acoustic modal parameters. Normal components of vibration displacement were obtained by experiments and used to calculate structural-acoustic modal coupling coefficients which determine the degree of coupling between structural mode and acoustic mode. The boundary panel, which contributes the most to the structural-acoustic modal coupling coefficients, was determined; then noise inside the vehicle was reduced by proper damping treatment and stiffness modification on that panel.

Acoustic sensitivity analysis of a car cab was performed by Ning et al. [4]. Both the structural and acoustical responses were calculated by FEM. They recommended decomposing acoustic sensitivity into magnitude and phase to obtain a trend with the change of SPL.

Davidson [5] studied vibro-acoustic problems with Finite Element (FE) model. He developed sub-structuring and modal reduction techniques for the solution of structural-acoustic problems for ease of computation. He also investigated effect of porous sound absorbing materials in FE model of vibro-acoustic systems.

Soenarko [6] applied single domain and multi domain BEM to predict noise spectrum between 500 Hz and 2500 Hz inside an automobile cabin excited by a point source at the corner. In multi domain approach, air inside the cabin, front and rear seats were modeled as different acoustic sub domains to consider the absorption of seat material. He compared the results with

measurements and concluded that multi domain method gave better results than single domain method.

Liu et al. [7] applied indirect BEM to find acoustic pressure inside a tracked vehicle having some open hatches on the chassis. Forces transmitted from the track system to chassis are determined using multi-body dynamic response analysis results. They performed dynamic response analysis of the chassis hull with FEM between 20 Hz and 280 Hz and determined vibration velocity of the panels to be used as boundary conditions for acoustic response analysis. Complex normal admittance boundary conditions were imposed to represent absorption of panels and A-weighted SPL was found at particular locations inside the vehicle. They mentioned in their study that BEM was accurate up to 264 Hz corresponding to an element size of one-sixth of shortest wavelength. The test results and analysis results were in good agreement up to 250 Hz.

Vlahopoulos and Allen [8] analyzed sound radiated from a structure which was randomly excited by boundary layer excitation. They utilized FEM and BEM integrated with stochastic analysis to predict the sound radiated from a simply supported plate excited by turbulent boundary layer.

Poro-elastic material behavior and its effect on acoustic field was studied using FEM-BEM coupling by Coyette [9]. It was stated that the intended use of poro-elastic layers on the structure is to absorb sound at low and medium frequencies. A porous screen and a structure having carpet, septum and fibrous layers were studied to find surface impedance as numerical

examples. Moreover, a plate with three layers of sheet metal, porous layer and heavy layer was analyzed to find transmission loss.

Cao and Deng [10] studied acoustic characteristics of a vehicle under engine and road excitation using coupled FEM and BEM. They investigated modal participation factor and panel acoustic contribution to make necessary changes in the design of a car for reduction of sound pressure level at the driver's right ear location.

İrfanoğlu [11] developed a computer code which has the capability of FEM-BEM coupling, to study interactions of structure and surrounding acoustic domain. In his thesis, case studies involving cavity backed problems were presented and compared with analytical solutions. Kopuz et al. [12-15]also studied vibro-acoustic coupling inside closed structures.

Finite Element Analysis (FEA) is the mostly used technique to find structural response of vehicle panels. The structural velocities are then taken as boundary conditions for the acoustic analysis. For the acoustic response FEM or BEM is preferred for low frequencies. Comparison of these two techniques is presented by Citarella et al. [16]. They made comparison of FEM-FEM model, FEM-BEM model and experimental results based on two indexes: the Frequency Response Scale Factor (FRSF) and the Frequency Response Assurance Criterion (FRAC). As a result of the comparison, FEM-BEM model gave closer results to experimental ones, compared to those of FEM-FEM model. To exercise more flexibility in FEM-BEM, they applied Modal Acoustic Transfer Vector (MATV) in their study. This approach eliminates solving system of equations each time the loading condition changes.

Kamçı et al. [17] implemented Modal Acoustic Transfer Vector (MATV) and Panel Acoustic Contribution Analysis (PACA) techniques to a vehicle model. They performed FEA for the structural response of the system and used the results as input to the BEM for the analysis of acoustic field. The excitation forces of the vehicle were the ones measured at the engine mounts for different engine speeds. Other excitations such as wind and tyre road interaction were neglected since they are associated with high frequency noise. Contribution of structural modes and contribution of each panel to acoustic response was studied with MATV and PACA approaches.

Wave Based Method (WBM) which uses exact solution of Helmholtz equation was studied by Desmet et al. [18-22]. It was shown that WBM is computationally more efficient than FEM and give better results at high frequencies since the size of WBM model is not as big as FEM model. The comparison of WBM, FEM and BEM for unbounded acoustic domain was given in these studies to show the convergence behavior of WBM.

Hal et al. [21] dealt with steady state acoustic problems with hybrid FEM-WBM which takes the advantage of computational efficiency of WBM and the capability of FEM to model complex geometries. Numerical example of 2D car cavity was presented which is compared with a FE model having a very fine mesh. It was reported that the convergence of the hybrid method depends on frequency. It converged to wrong values at low frequencies, however; at mid and high frequencies this method was more accurate and more efficient.

Hybrid FEM-WBM was compared with FEM-FEM method by Genechten et al. [23]. The FEM mesh size, number of wave equations used in analysis and truncation effects were studied on a cavity backed steel plate example.

Charpentier et al. [24] used hybrid SEA and FEM to analyze structure-borne noise and air-borne noise of a vehicle between 200 Hz to 1 kHz. Rigid components are modeled with FEM and other components having high modal density are modeled with SEA subsystems. The vibration analysis results were validated with impact hammer tests on the panels, on the right axle and on the engine mounts. Also, acoustic response results were validated with experiments and the difference of experimental and numerical results were found to be less than 5 dB. Cotoni et al. [25] discovered that smooth shaped panels have lower radiation efficiency than complex shaped panels.

Noise spectra of products are also investigated from different aspects, such as virtual noise synthesis or experimental methods. Pavic [26] studied contributions of various noise sources to the overall noise level of industrial products by combining experimental results of noise sources with the model of the frame. It was explained that the transfer functions from each noise generating structure together with the effect of frame to the noise are used in noise synthesis. Modeling of air-borne and structure-borne noises was illustrated by an example for a household refrigerator. Ramsey and Firmin [27] explained the procedure that can be followed to solve noise and vibration problem of a structure. He suggested obtaining modal model by experimentally detecting resonance frequencies and mode shapes. Structural dynamic modification techniques were applied to find structural response

after some modifications. This method was compared with FEM and found to be more efficient since the number of degrees of freedom was less and FEM under-estimated the resonance frequencies. Guimaraes and Medeiros [28] conducted experiments to study the acoustic pressure at the driver's ear position considering both structure and air-borne sources. Contribution of each source was obtained and combined with Transfer Path Analysis (TPA).

Crowley et al. [29] used experimentally obtained frequency response functions of original structure and applied direct structural modification technique. This technique was also used to validate modal models obtained from experimental data.

A method for structural damping modifications by using matrix inversion and its extension to find damped receptances of non-proportionally damped structures from undamped counterparts by avoiding matrix inversion were proposed by Özgüven [30]. In that study addition of modifications impose no additional degrees of freedom to the original structure. Later, Özgüven [1] generalized the structural modification method for any type of modification in the system and furthermore extended the method for cases; with additional degrees of freedom; that is for coupling problems. In both cases the dimension of matrix to be inverted was limited to degrees of freedom related to modification locations.

Köksal et al. [31] used the equations given in Özgüven's Structural Modification Method [1] and avoided matrix inversion by power series expansion. In a later study, Köksal et al. [32] compared computational efficiency of the three structural modification methods; Özgüven's Structural

Modification Method, Structural Modification Method by Using Sherman-Morrison Formula and Extended Successive Matrix Inversion Method. All three methods use the frequency response functions (FRFs) of original structure; and also mass, stiffness and damping matrices of modifying structure. Three case studies were presented and Özgüven's Structural Modification Method was found to be the most efficient method among the three.

Alan et al. [33] used the Matrix Inversion Method by Özgüven [1] to predict the workpiece dynamics during a complete machining cycle of a workpiece for chatter stability analysis.

Başdoğan et al. [34] presented vibro-acoustic results of structural modification on a mid panel of a rectangular structure. In the study, structural modification technique for distributed modifications, explained by Canbaloğlu and Özgüven [35], was used and acoustic pressure at a point inside the structure was found by BEM using the acoustic transfer vector (ATV) approach.

1.3 Motivation and Scope of the Thesis

The motivation behind this study is to find a fast and an efficient solution in structural modification problems of vibro-acoustic systems. It is important to determine the optimum location and geometry of modifying elements to get the lowest sound pressure levels at desired points. For this purpose, structural modification technique by Özgüven is integrated with the vibro-

acoustic analysis using coupled FEM/BEM method. Different case studies are carried out to examine the effectiveness of this method.

The outline of the dissertation is given below:

In Chapter 2, theoretical background of the subject is explained. Structural modification techniques are presented. Then, numerical methods used in noise level prediction are explained. Vibro-acoustic approach for structure and acoustic medium interaction is given as FEM-FEM coupling and FEM-BEM coupling.

In Chapter 3, application procedure of structural modifications with additional degrees of freedom is given in detail. The application is also shown with different case studies.

In Chapter 4, procedure of BEM to obtain noise level inside closed structures is given. Two case studies are presented for unmodified structure and modified structure to illustrate the effect of structural excitation on the walls of the rectangular cavity to sound pressure. Then, acoustic excitation by a point source inside a rectangular cavity is studied.

In Chapter 5, FEA is performed for a rectangular structure and structural modifications are applied on the structure. The structural modification is carried by adding stiffeners. The response of the structure is carried by structural modification technique and imported to the boundary element analysis program as boundary conditions. The effects of stiffener geometry and position are investigated.

In Chapter 6, the results are discussed; conclusion of the study is given. Moreover, suggestions for future work in this area are also studied.

CHAPTER 2

THEORY

2.1 Structural Modification Technique

Optimum design of products requires changes on the structure. Numerical models are frequently employed for the analysis of structures, and the behavior of the structure under different loads can be predicted before the production phase. However; reanalysis of big and complex structures after every modification may be a time consuming process.

The structural modification techniques presented in the following sections require the receptance matrix of the original structure and dynamic stiffness matrix of the modifying structure. These methods give exact values of receptances for the modified structure if exact receptances of original structure are used in the calculations [1].

In this part, structural modification is investigated under two headings/sub-titles; namely, structural modifications without additional degrees of freedom and with additional degrees of freedom.

2.1.1 Structural Modifications without Additional Degrees of Freedom

System response after structural modifications that do not impose additional degrees of freedom was obtained by Özgüven [1].

The response of a system with stiffness matrix $[K]$, mass matrix $[M]$ and structural damping matrix $[H]$ is represented by

$$\{x\} = \left[[K] - \omega^2 [M] + i[H]\right]^{-1} \{F\} \tag{2.1}$$

The receptance matrix of the unmodified structure can be written by

$$[\alpha] = \left[[K] - \omega^2 [M] + i[H]\right]^{-1} \tag{2.2}$$

The dynamic stiffness matrix of the modifying structure denoted by $[D]$ is

$$[D] = [\Delta K] - \omega^2 [\Delta M] + i[\Delta H] \tag{2.3}$$

where $[\Delta K]$, $[\Delta M]$ and $[\Delta H]$ are stiffness, mass and structural damping matrices of the modifying structure, respectively. The receptance matrix of the modified structure is then expressed by

$$[\gamma] = \left[\left[[K] + [\Delta K]\right] - \omega^2 \left[[M] + [\Delta M]\right] + i\left[[H] + [\Delta H]\right]\right]^{-1} \tag{2.4}$$

Combining equations (2.2) and (2.4) yields

$$[\gamma]^{-1} = [\alpha]^{-1} + [D] \tag{2.5}$$

Both sides of equation (2.5) is pre-multiplied by $[\alpha]$ and post multiplied by $[\gamma]$ to obtain

$$[\alpha]=[\gamma]+[\alpha][D][\gamma] \tag{2.6}$$

Rearranging equation (2.6) yields

$$[\alpha]=\left[[I]+[\alpha][D]\right][\gamma] \tag{2.7}$$

Then, $[\gamma]$ is obtained as

$$[\gamma]=\left[[I]+[\alpha][D]\right]^{-1}[\alpha] \tag{2.8}$$

Assuming the structural modification is local, structural modification matrix $[D]$ can be written as

$$[D]=\begin{bmatrix}[D_{11}] & [0]\\ [0] & [0]\end{bmatrix} \tag{2.9}$$

The receptance matrix of the modified system in partitioned form can be obtained as

$$[\gamma_{11}]=\left[[I]+[\alpha_{11}][D_{11}]\right]^{-1}[\alpha_{11}] \tag{2.10}$$

$$[\gamma_{21}]=[\alpha_{21}]\left[[I]-[D_{11}][\gamma_{11}]\right]=[\gamma_{12}]^{T} \tag{2.11}$$

$$[\gamma_{22}]=[\alpha_{22}]-[\alpha_{21}][D_{11}][\gamma_{12}] \tag{2.12}$$

where subscript 1 denotes modified regions and subscript 2 stands for unmodified regions of the structure. As seen in equation (2.10) overall size of the matrix to be inverted is equal to the size of modified degrees of freedom which decreases the computational time in the analysis.

In this approach, addition of a new element does not add a new degree of freedom to the system which is illustrated in Figure 2.1. The inertia terms of original and modifying structures are simply added to find inertias in the mass matrix for the modified structure. However, the inertia of modified structure is not the sum of original and modifying structures' inertias which is shown in equation (2.13). To get rid of this problem, structural modifications with additional degrees of freedom technique can be applied.

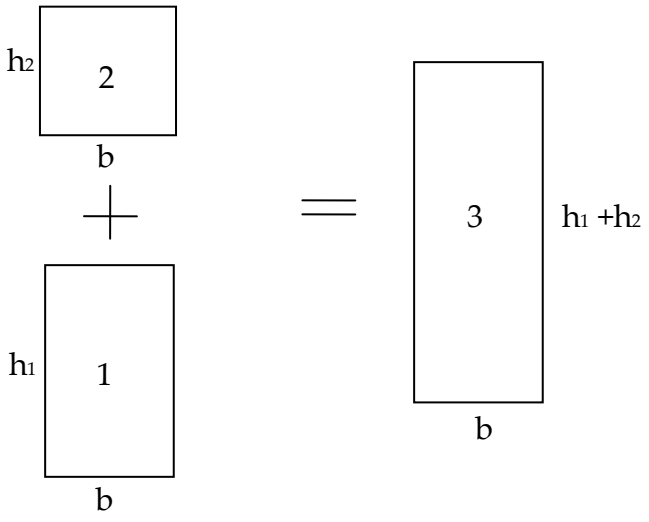

Figure 2.1 Addition of two elements

$$I_1 = \frac{bh_1^3}{12}$$
$$I_2 = \frac{bh_2^3}{12} \tag{2.13}$$
$$I_3 = \frac{b\left(h_1 + h_2\right)^3}{12} \neq \frac{bh_1^3}{12} + \frac{bh_2^3}{12}$$

2.1.2 Structural Modifications with Additional Degrees of Freedom

System response after structural modifications with additional degrees of freedom was developed by Özgüven [1]. The idea is similar to the previous one. In this case, the modifying elements are considered as new elements with different degrees of freedom. Using equation(2.5), receptance matrix of the modified structure can be written as

$$\begin{bmatrix} \gamma_{aa} & \gamma_{ab} & \gamma_{ac} \\ \gamma_{ba} & \gamma_{bb} & \gamma_{bc} \\ \gamma_{ca} & \gamma_{cb} & \gamma_{cc} \end{bmatrix}^{-1} = \begin{bmatrix} [\alpha]^{-1} & & 0 \\ & & 0 \\ 0 & 0 & 0 \end{bmatrix} + \begin{bmatrix} 0 & 0 & 0 \\ 0 & & \\ 0 & & [D] \end{bmatrix} \tag{2.14}$$

where $[D]$ is given in equation (2.3). Subscript *a* corresponds to degrees of freedom which belong only to original structure, *b* corresponds to degrees of freedom associated to both original structure and modifying structure (common degrees of freedom) and *c* represents the degrees of freedom belonging only to modifying structure

$$[\alpha]^{-1} = \begin{bmatrix} \alpha_{aa} & \alpha_{ab} \\ \alpha_{ba} & \alpha_{bb} \end{bmatrix}^{-1} = [K] - \omega^2 [M] + i[H] \tag{2.15}$$

Pre-multiplying equation (2.14) by

$$\begin{bmatrix} [\alpha] & \begin{matrix}0\\0\end{matrix} \\ \begin{matrix}0 & 0\end{matrix} & I \end{bmatrix} \tag{2.16}$$

and post-multiplying by $[\gamma]$ yields

$$\begin{bmatrix} [\alpha] & \begin{matrix}0\\0\end{matrix} \\ \begin{matrix}0 & 0\end{matrix} & I \end{bmatrix} = \begin{bmatrix} I & 0 & 0 \\ 0 & I & 0 \\ 0 & 0 & 0 \end{bmatrix} [\gamma] + \left[\begin{array}{c|cc} 0 & [\alpha_{ab}] & 0 \\ \hline 0 & \multicolumn{2}{c}{\multirow{2}{*}{$\begin{bmatrix} \alpha_{bb} & 0 \\ 0 & I \end{bmatrix} \cdot [D]$}} \\ 0 & & \end{array}\right] [\gamma] \tag{2.17}$$

After some matrix manipulations, it is possible to obtain

$$\left[\begin{bmatrix} I & 0 \\ 0 & 0 \end{bmatrix} + \begin{bmatrix} \alpha_{bb} & 0 \\ 0 & I \end{bmatrix} \cdot [D] \right] \begin{bmatrix} \gamma_{ba} \\ \gamma_{ca} \end{bmatrix} = \begin{bmatrix} \alpha_{ba} \\ 0 \end{bmatrix} \tag{2.18}$$

$$\left[\begin{bmatrix} I & 0 \\ 0 & 0 \end{bmatrix} + \begin{bmatrix} \alpha_{bb} & 0 \\ 0 & I \end{bmatrix} \cdot [D] \right] \begin{bmatrix} \gamma_{bb} & \gamma_{bc} \\ \gamma_{cb} & \gamma_{cc} \end{bmatrix} = \begin{bmatrix} \alpha_{bb} & 0 \\ 0 & I \end{bmatrix} \tag{2.19}$$

$$[\gamma_{aa}] + [\alpha_{ab} \mid 0][D] \begin{bmatrix} \gamma_{ba} \\ \gamma_{ca} \end{bmatrix} = [\alpha_{aa}] \tag{2.20}$$

$$[\gamma_{ab} \mid \gamma_{ac}] + [\alpha_{ab} \mid 0][D] \begin{bmatrix} \gamma_{bb} & \gamma_{bc} \\ \gamma_{cb} & \gamma_{cc} \end{bmatrix} = [\alpha_{ab} \mid 0] \tag{2.21}$$

Using equations (2.18), (2.19), (2.20) and (2.21), the receptance matrix of modified structure, $[\gamma]$ is obtained. It is possible to write $[\gamma]$ in terms of the receptance matrix of original structure, $[\alpha]$, and dynamic stiffness matrix of the modifying structure, $[D]$,

$$\begin{bmatrix}\gamma_{ba}\\ \gamma_{ca}\end{bmatrix}=\left[\begin{bmatrix}I & 0\\ 0 & 0\end{bmatrix}+\begin{bmatrix}\alpha_{bb} & 0\\ 0 & I\end{bmatrix}\cdot[D]\right]^{-1}\begin{bmatrix}\alpha_{ba}\\ 0\end{bmatrix} \tag{2.22}$$

$$\begin{bmatrix}\gamma_{bb} & \gamma_{bc}\\ \gamma_{cb} & \gamma_{cc}\end{bmatrix}=\left[\begin{bmatrix}I & 0\\ 0 & 0\end{bmatrix}+\begin{bmatrix}\alpha_{bb} & 0\\ 0 & I\end{bmatrix}\cdot[D]\right]^{-1}\begin{bmatrix}\alpha_{bb} & 0\\ 0 & I\end{bmatrix} \tag{2.23}$$

$$[\gamma_{aa}]=[\alpha_{aa}]-[\alpha_{ab}\ \vdots\ 0][D]\begin{bmatrix}\gamma_{ba}\\ \gamma_{ca}\end{bmatrix} \tag{2.24}$$

$$[\gamma_{ab}\ \vdots\ \gamma_{ac}]=[\alpha_{ab}\ \vdots\ 0]\left[[I]-[D]\begin{bmatrix}\gamma_{bb} & \gamma_{bc}\\ \gamma_{cb} & \gamma_{cc}\end{bmatrix}\right] \tag{2.25}$$

2.2 Numerical Methods Used in Noise Level Prediction

Analytical solution of acoustic problems for complex shaped domains is difficult to perform, so numerical solution techniques are developed for acoustic analysis of such domains. First, acoustic wave equation which describes the motion of fluid particles under the effect of acoustic wave is derived basically. The field variables of fluid when disturbed by the acoustical perturbation are [36]

$$P = p_0 + p \tag{2.26}$$

$$\underline{\rho} = \rho_0 + \rho \tag{2.27}$$

where P is total pressure, p_0 is equilibrium pressure of the medium, p is the acoustic pressure, $\underline{\rho}$ is the total density, ρ_0 is the equilibrium density of the medium and ρ is the density change.

Assumptions used in the derivation of wave equation can be listed as

- ✓ Medium is perfectly elastic, isotropic and homogeneous
- ✓ Effects of body forces are neglected
- ✓ Equilibrium pressure and density, p_0 and ρ_0, are uniform throughout the medium owing to negligence of body forces
- ✓ All dissipative effects due to viscosity and heat conduction are neglected
- ✓ Waves have small amplitudes such that density changes with respect to ρ_0 are small.

Conservation of mass, equation of motion, conservation of energy and equation of state are combined to obtain acoustic wave equation as

$$\frac{1}{c^2}\frac{\partial^2 p}{\partial t^2} - \nabla^2 p = 0 \tag{2.28}$$

where $\nabla^2 = \frac{\partial^2}{\partial x^2} + \frac{\partial^2}{\partial y^2} + \frac{\partial^2}{\partial z^2}$ is 3D Laplacian operator. Solution of unforced wave equation gives distribution of pressure field in the acoustic medium. If the acoustic pressure fluctuation is assumed to be harmonic $p = \hat{p}e^{j\omega t}$, Helmholtz equation is obtained as

$$\nabla^2 \hat{p} + k^2 \hat{p} = 0 \tag{2.29}$$

where $k = \omega/c$ is wave number.

In the following sub-sections, FEM, SEA and BEM are explained. FEM and BEM are deterministic methods, whereas SEA is a probabilistic method.

2.2.1 Finite Element Method (FEM)

The dynamic behavior of the acoustic pressure inside a closed cavity can be modeled by FEM using acoustic wave equation. FEM is based on transformation of the original problem into an equivalent integral formulation. Shape functions are defined within finite elements for the approximation of field variables and geometry of the domain. In a weighted residual method, trial shape functions are used to build solution for each field variable. In the variational method the exact distributions of the field variables are defined instead of trial shape functions [37].

In order to get nonhomogeneous wave equation source term, q (added mass per unit volume) is added to wave equation (2.28) as [38]

$$\frac{1}{c^2}\frac{\partial^2 p}{\partial t^2} - \nabla^2 p = \frac{\partial q}{\partial t} \tag{2.30}$$

FEM formulation is obtained by multiplying (2.30) by a test function υ_F and integrating over fluid volume V_F

$$\int_{V_F} \upsilon_F \left(\frac{1}{c^2}\frac{\partial^2 p}{\partial t^2} - \nabla^2 p - \frac{\partial q}{\partial t} \right) dV = 0 \tag{2.31}$$

and applying Green's theorem and introducing shape functions, N_F, give finite element formulation for acoustic domain as

$$\int_{V_F} {N_F}^T N_F dV\ddot{p} + c^2 \int_{V_F} \left(\nabla N_F\right)^T \nabla N_F dVp = c^2 \int_{\partial V_F} {N_F}^T \nabla p n_F dS + c^2 \int_{V_F} {N_F}^T \frac{\partial q}{\partial t} dV \quad (2.32)$$

where n_F is boundary normal vector pointing outward from the domain,

The system of equations are obtained as

$$M_F \ddot{p} + K_F p = f_q + f_S \quad (2.33)$$

where

$$\begin{aligned} M_F &= \int_{V_F} {N_F}^T N_F dV \\ K_F &= c^2 \int_{V_F} \left(\nabla N_F\right)^T \nabla N_F dV \\ f_S &= c^2 \int_{\partial V_F} {N_F}^T \nabla p n_F dS \\ f_q &= c^2 \int_{V_F} {N_F}^T \frac{\partial q}{\partial t} dV \end{aligned} \quad (2.34)$$

FEM requires 3D discretization of the domain which yields very large, sparsely populated system matrices to be solved.

2.2.2 Boundary Element Method (BEM)

BEM is an alternative deterministic method which has some advantages over FEM. One of the advantages of BEM over FEM is that it can be applied to both bounded and unbounded domains. Infinite domains are easily handled using BEM especially for exterior acoustic analysis. Moreover, only the boundaries of domain are discretized in BEM so the dimensionality reduces

by one. Besides, mesh generation is easy since only the boundaries of the domain are meshed. In other words it is simple in geometric modeling. However, system matrices in BEM are fully populated and unsymmetrical which requires unsymmetrical solvers for the analysis.

To get an integral equation for the BEM, special functions called fundamental solutions are used. For acoustic problems in frequency domain, first fundamental solution, namely free-space Green's function, is used and it satisfies Helmholtz equation in unbounded domain when there is a concentrated unit excitation at source point [11]. At the surface $G(r, r_s)$ satisfies point source equation

$$k^2 G(r, r_s) + \nabla^2 G(r, r_s) = -\delta(r - r_s) \tag{2.35}$$

where $\delta(r - r_s)$ is Dirac's Delta function where r is a point inside the domain and r_s is a point on the surface. The domain nomenclature is shown in Figure 2.2. The solution of the differential equation gives [39]

$$G(r, r_s) = -\frac{e^{ik|r - r_s|}}{4\pi |r - r_s|} \tag{2.36}$$

Other fundamental solutions are listed in reference [39] .

Green's Second Identity is used in the derivation of the integral equation and it is expressed as

$$\int_V \left[T\nabla^2 U - U\nabla^2 T \right] dV = \int_S \left(T \frac{\partial U}{\partial \upsilon} - U \frac{\partial T}{\partial \upsilon} \right) dS \tag{2.37}$$

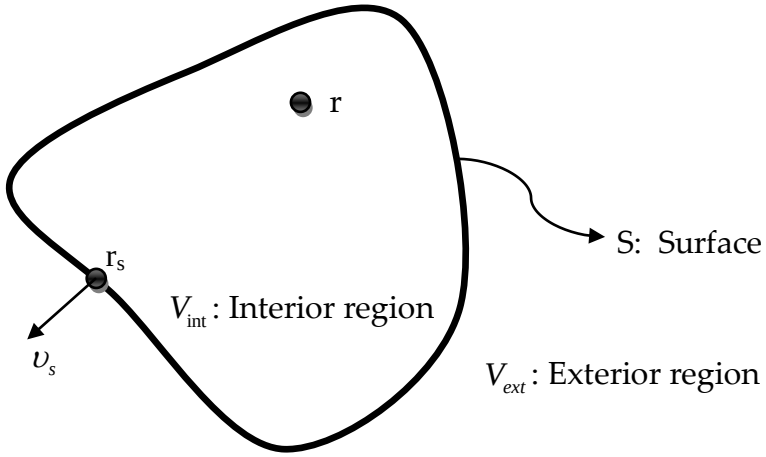

Figure 2.2 Domain nomenclature for BEM

Replacing T and U by $\hat{p}(r_s)$ and $G(r,r_s)$, respectively and rearranging equation (2.37) yields

$$\int_V \left[\nabla^2 G(r,r_s) + G(r,r_s)k^2 \right] \hat{p} dV = \int_S \left(\hat{p}(r_s) \frac{\partial G(r,r_s)}{\partial \upsilon_s} - G(r,r_s) \frac{\partial \hat{p}(r_s)}{\partial \upsilon_s} \right) dS \quad (2.38)$$

where υ_s is the outward normal vector of the surface of the acoustic domain. Substituting equation (2.35) gives Helmholtz integral equation for interior acoustic domains as [40]

$$\int_S \left(\hat{p}(r_s) \frac{\partial G(r,r_s)}{\partial \upsilon_s} - G(r,r_s) \frac{\partial \hat{p}(r_s)}{\partial \upsilon_s} \right) dS = \begin{cases} 0 & r \in V_{ext} \\ -\hat{p}(r) & r \in V_{\text{int}} \\ -\dfrac{\hat{p}(r)}{2} & r \in S \end{cases} \quad (2.39)$$

Similarly, for exterior domains, Helmholtz integral can be written as

$$\int_S \left(\hat{p}(r_s) \frac{\partial G(r, r_s)}{\partial \upsilon_s} - G(r, r_s) \frac{\partial \hat{p}(r_s)}{\partial \upsilon_s} \right) dS = \begin{cases} \hat{p}(r) & r \in V_{ext} \\ 0 & r \in V_{\text{int}} \\ \dfrac{\hat{p}(r)}{2} & r \in S \end{cases} \tag{2.40}$$

To solve the integral equation, boundary conditions should be specified for the medium under consideration. For the case in which acoustic field inside a cavity is considered, in other words for interior acoustic problem, boundary conditions can be expressed using either acoustic pressure or normal component of acoustic particle velocity or combination of the two variables. At a surface point;

$$\frac{\partial \hat{p}}{\partial \upsilon_s} = -i\omega\rho_0 \vartheta_n \tag{2.41}$$

where ϑ_n is normal velocity component. Possible boundary conditions for the solution of Helmholtz integral for interior acoustic analysis are

- Rigid Boundary

$$\frac{\partial \hat{p}(r_s)}{\partial \upsilon_s} = 0 \tag{2.42}$$

- Pressure Release

$$\hat{p}(r_s) = 0 \tag{2.43}$$

- Impedance Surface

$$\frac{\partial \hat{p}(r_s)}{\partial \upsilon_s} = -i\omega\rho_0 \vartheta_n \tag{2.44}$$

- Vibrating surface

$$\frac{\partial \hat{p}(r_s)}{\partial \upsilon_s} = \omega^2 \rho_0 d_n \tag{2.45}$$

where d_n is displacement of the vibrating surface in the direction of surface normal.

2.2.2.1 Classical BEM

In this part direct and indirect formulations for the BEM are presented. Direct BEM can be accomplished with the method of weighted residuals or with Green's second identity. Indirect formulation is developed by using single and double layer potentials.

2.2.2.1.1 Direct BEM

Direct formulation of BEM applies pressure and normal velocity on boundary surfaces as boundary condition. Direct formulation using Green's second identity is presented in this part.

The influence matrices ($[A(\omega)]$ and $[B(\omega)]$) are non-symmetric, fully populated and frequency dependent. The system of equations can be written as [41]

$$[A(\omega)]\{p\} = [B(\omega)]\{\vartheta_n\} \tag{2.46}$$

The acoustic pressure expression for direct method is expressed as [9]

$$p(x) = \int_S \left\{ p(y) \frac{\partial G(x,y)}{\partial \upsilon_s} - \frac{\partial p(x,y)}{\partial \upsilon_s} G(x,y) \right\} dS(y) \tag{2.47}$$

Direct formulation can only be applied for closed domains. If there are openings on the domain indirect formulation should be adopted to analyze the problem.

2.2.2.1.2 Indirect BEM

Indirect BEM uses pressure and normal velocity discontinuities at the surface as boundary conditions. The resulting system matrices are fully populated and symmetric. The system of equations for indirect formulation are as follows [41]

$$\begin{bmatrix} B & C^T \\ C & D \end{bmatrix} \begin{Bmatrix} \sigma \\ \tau \end{Bmatrix} = \begin{Bmatrix} f \\ g \end{Bmatrix} \tag{2.48}$$

where σ and τ represents a jump of velocity (single layer potential) and jump of pressure (double layer potential), respectively. Also, f and g are the

excitation vectors. B, C and D are the influence matrices which depend on the shape fuctions and Green's function [13].

This feature is useful for structures having openings to the outside. It can be applied to both interior and exterior domains. Acoustic pressure at any point can be calculated using [9]

$$p(x) = \int_S \left\{ \tau(y) \frac{\partial G(x,y)}{\partial \upsilon_s} - \sigma(y) G(x,y) \right\} dS(y) \tag{2.49}$$

2.2.2.2 Wave Based Method (WBM)

WBM is a variation of BEM which uses wave functions that are exact solutions of the Helmholtz equation to approximate dynamic acoustic field. The model matrices are complex and fully populated since wave functions are complex functions. It is a deterministic method based on indirect Trefftz approach and it is applicable to mid-frequency problems. It does not require fine meshes and the computation time decreases. Acoustic pressure is approximated as [20].

$$p(x,y,z) \approx \sum_{a=1}^{n_a} p_a \Phi_a(x,y,z) \tag{2.50}$$

where $\Phi_a(x,y,z)$ is an acoustic wave function which is one of

$$\begin{cases} \Phi_{ar}(x,y,z) = \cos(k_{xa_r} x)\cos(k_{ya_r} y) e^{-jk_{xa_r} z} \\ \Phi_{as}(x,y,z) = \cos(k_{xa_s} x) e^{-jk_{ya_s} y} \cos(k_{za_s} z) \\ \Phi_{at}(x,y,z) = e^{-jk_{xa_t} x} \cos(k_{ya_t} y)\cos(k_{za_t} z) \end{cases} \tag{2.51}$$

Infinite number of wave functions can be defined, however; it is proposed to use the following wave numbers

$$\left(k_{xa_r}, k_{ya_r}, k_{za_r}\right) = \left(\frac{a_1\pi}{L_x}, \frac{a_2\pi}{L_y}, \pm\sqrt{k^2 - \left(\frac{a_1\pi}{L_x}\right)^2 - \left(\frac{a_2\pi}{L_y}\right)^2}\right)$$
$$\left(k_{xa_s}, k_{ya_s}, k_{za_s}\right) = \left(\frac{a_3\pi}{L_x}, \pm\sqrt{k^2 - \left(\frac{a_3\pi}{L_x}\right)^2 - \left(\frac{a_4\pi}{L_z}\right)^2}, \frac{a_4\pi}{L_z}\right) \quad (2.52)$$
$$\left(k_{xa_t}, k_{ya_t}, k_{za_t}\right) = \left(\pm\sqrt{k^2 - \left(\frac{a_5\pi}{L_y}\right)^2 - \left(\frac{a_6\pi}{L_z}\right)^2}, \frac{a_5\pi}{L_y}, \frac{a_6\pi}{L_z}\right)$$

where $a_1, a_2, a_3, a_4, a_5, a_6 = 0,1,2\ldots$ and L_x, L_y, L_z are the dimensions of enclosed fluid domain in Cartesian directions.

Similarly, this approach can be applied for structural domain. Structural wave functions are used which satisfies homogeneous part of the fourth order dynamic plate equation. Structure and acoustic coupling using WBM is explained in detail in [20, 22].

2.2.3 Statistical Energy Analysis (SEA)

SAE is a probabilistic method which is developed for high frequency analysis with high modal densities. The original system is examined as composed of subsystems which have probabilistic parameters. Vibration behavior of the system is expressed in terms of the time average total vibration energy of each subsystem. Excitation is defined as time-average input powers [42].

Some of the input energy is dissipated within the subsystem and the rest is transferred to the neighboring subsystems. This can be expressed as [2]

$$[\Pi] = \omega[L]\cdot[E] \tag{2.53}$$

where $[\Pi]$ represents input powers, $[\omega]$ is center frequency of band under consideration, $[L]$ contains internal loss factors and coupling loss factors and $[E]$ represents subsystem energies. $[E]$ can be found if input power $[\Pi]$ and loss factor matrix $[L]$ are known. The equation may also be written as

$$\begin{bmatrix} \Pi_1 \\ \cdots \\ \Pi_k \end{bmatrix} = \omega \begin{bmatrix} R_1 + \sum_{i\neq 1} R_{1i} & -R_{12} & -R_{1k} \\ \cdots & \cdots & \cdots \\ -R_{k1} & -R_{k2} & R_k + \sum_{i\neq 1} R_{ki} \end{bmatrix} \begin{bmatrix} \frac{E_1}{n_1} \\ \cdots \\ \frac{E_k}{n_k} \end{bmatrix} \tag{2.54}$$

where R_{ij} is power transfer coefficient expressed as $\eta_{ij}\omega n_i$, η_{ij} is coupling loss factor between sub-systems *i* and *j*. R_i is power transfer coefficient expressed as $\eta_i\omega n_i$, η_i is subsystem damping loss factor and n_i is sub-system modal density defined as number of modes per frequency of unit Herz. There are three modes in which equation (2.54) is used [42], such that

- input power distributions, $[\Pi]$, and power transfer coefficients, $\omega[L]\cdot[n]$, are known or assumed, then elements of $[E]/[n]$ matrix are obtained by inverting the power transfer coefficients
- assuming power transfer coefficients are invariant with respect to the distribution of external input power to the subsystems, input powers

are applied to each sub-system, total energies of all the sub-systems are estimated using dissipation loss factors and coupling loss factors. This is not a feasible approach since the power transfer coefficient matrix cannot be determined directly without the knowledge of modal densities

- principal power transmission paths between multiply connected subsystems are identified by setting relative modal energies as experimental estimates

Modal densities, coupling loss factors, and power input are determined either by theoretically or by empirically. Damping loss factors can be assumed to be constant for all modes which lead to uncertainty in the analysis. On the other hand damping loss factors of sub-systems can be found empirically. Space averaged vibration velocities, $\langle v^2 \rangle$, and space averaged sound pressures, $\langle p^2 \rangle$, are found by [2]

$$E_{structure} = m\langle v^2 \rangle \tag{2.55}$$

$$E_{acoustic} = V\frac{\langle p^2 \rangle}{\langle \rho_0 c^2 \rangle} \tag{2.56}$$

where m is mass of the subsystem, V is subsystem volume, ρ_0 is density of medium and c is speed of sound for the medium.

An advantage of SEA is that degrees of freedom of subsystems are low compared to FEA, so computational effort is less. Moreover, it allows predicting upper limit for the response of the system. However, at low

frequencies where modal density is low, SEA does not give reliable results. For instance, modal density of acoustic cavity inside vehicles is very low at low frequencies; so SEA is not preferred for low frequency booming noise predictions. Instead, new hybrid methods combining SEA and FEA are developed for vibro-acoustic analysis to comprise broader frequency ranges [24]. Another disadvantage of SEA is the uncertainty in the results since it is a probabilistic method.

2.3 Numerical Methods for Vibro-Acoustic Problems

Sound generation by vibration of surface of a structure is studied in vibro-acoustic field of engineering. The fluid particles in the acoustic medium, air, show small local perturbations due to vibration of the structure surface in contact. Compression and rarefaction zones occur with a wave length which depends on the speed of propagation and the frequency of vibration [43]. These pressure perturbations in the acoustic medium, air, contributes to the sound we hear.

In order to compute acoustic pressure at a point, vibration response of the structure is needed as boundary conditions for acoustic medium. The coupling depends on the interaction between the two domains. In other words, strong coupling exists if the acoustic pressure exerts load on the structure and the structure's velocity defines the acoustic velocity on the acoustic domain. On the other hand, weak coupling or one way coupling covers situations where structure dynamics is not influenced by the acoustic fluid. If both the structure and acoustic medium are modeled using finite elements, it is named as FEM-FEM coupling. If the structure is modeled

using finite elements and the boundaries of the acoustic domain are modeled by boundary elements, it is called FEM-BEM coupling. In the following sections, FEM-FEM coupling and FEM-BEM coupling are explained.

2.3.1 FEM-FEM Coupling

Governing equations for structural domain are [44]

$$M_s\ddot{d}_s + K_s d_s = f_F + f_b \tag{2.57}$$

where

$$\begin{aligned} M_S &= \int_{V_S} N_S{}^T \rho_S N_S dV \\ K_S &= c^2 \int_{V_S} \left(\tilde{\nabla} N_S\right)^T D_S \tilde{\nabla} N_S dV \\ f_F &= \int_{\partial V_S} N_S{}^T t_S dS \\ f_b &= \int_{V_S} N_S{}^T b_S dV \end{aligned} \tag{2.58}$$

where t_S is surface traction vector, b_S represent body forces, ρ_S is the density of structure material and N_S are structural shape functions. Differential operator $\tilde{\nabla}$ and constitutive matrix D_S are expressed as

$$\tilde{\nabla} = \begin{bmatrix} \frac{\partial}{\partial x_1} & 0 & 0 \\ 0 & \frac{\partial}{\partial x_2} & 0 \\ 0 & 0 & \frac{\partial}{\partial x_3} \\ \frac{\partial}{\partial x_2} & \frac{\partial}{\partial x_1} & 0 \\ \frac{\partial}{\partial x_3} & 0 & \frac{\partial}{\partial x_1} \\ 0 & \frac{\partial}{\partial x_3} & \frac{\partial}{\partial x_2} \end{bmatrix} \tag{2.59}$$

$$D_S = \begin{bmatrix} \lambda+2\mu & \lambda & \lambda & 0 & 0 & 0 \\ \lambda & \lambda+2\mu & \lambda & 0 & 0 & 0 \\ \lambda & \lambda & \lambda+2\mu & 0 & 0 & 0 \\ 0 & 0 & 0 & \mu & 0 & 0 \\ 0 & 0 & 0 & 0 & \mu & 0 \\ 0 & 0 & 0 & 0 & 0 & \mu \end{bmatrix} \tag{2.60}$$

where the Lame coefficients, λ and , μ are expressed in the modulus of elasticity, E, the shear modulus, G, and Poisson's ratio, υ by

$$\lambda = \frac{\upsilon E}{(1+\upsilon)(1-2\upsilon)}$$
$$\mu = G = \frac{E}{2(1+\upsilon)} \tag{2.61}$$

At the structure-fluid interface, fluid particles and the surface of structure move in the normal direction to the boundary surface, so the normal velocities at the boundary are taken equal for coupling. Also the pressure at

the interface is equal for both fluid and the structure. Applying these two boundary conditions yield unsymmetrical system of equations [5]

$$\begin{bmatrix} M_s & 0 \\ \rho_0 c^2 H^T & M_f \end{bmatrix} \begin{bmatrix} \ddot{d}_s \\ \ddot{p} \end{bmatrix} + \begin{bmatrix} K_s & -H \\ 0 & K_f \end{bmatrix} \begin{bmatrix} d_s \\ p \end{bmatrix} = \begin{bmatrix} f_b \\ f_q \end{bmatrix} \tag{2.62}$$

where H is the spatial coupling matrix

$$H = \int_{\partial V_{SF}} N_S{}^T n N_f \, dS \tag{2.63}$$

n is the normal vector $n = n_f = -n_S$.

2.3.2 FEM-BEM Coupling

Introducing the structure coupling boundary condition to the Helmholtz integral equation, the pressure on the surface of a vibrating body is expressed in integral form [43]

$$\int_S \left(\hat{p}(r_s) \frac{\partial G(r, r_s)}{\partial \upsilon_s} - G(r, r_s) \omega^2 \rho_0 u_n \right) dS = -\frac{\hat{p}(r)}{2} \tag{2.64}$$

The pressure on the surface S is evaluated solving the equation (2.64) for point r on the surface. Then, knowing the pressure on the surface of the body, $\hat{p}(r_s)$, the pressure at any point in the volume, $\hat{p}(r)$ can be evaluated using equation (2.39).

System of equations for structural FEM- acoustic indirect BEM can be expressed as [41]

$$\begin{bmatrix} K_S - \omega^2 M_S & C^t \\ C & \dfrac{H(\omega)}{\rho_0 \omega^2} \end{bmatrix} \begin{Bmatrix} d_s \\ \mu \end{Bmatrix} = \begin{Bmatrix} F_S \\ \dfrac{F_A}{\rho_0 \omega^2} \end{Bmatrix} \tag{2.65}$$

Similarly, system of equations for structural FEM- acoustic direct BEM can be expressed as [41]

$$\begin{bmatrix} K_S - \omega^2 M_S & C^t \\ \rho_0 \omega^2 B(\omega) & A(\omega) \end{bmatrix} \begin{Bmatrix} d_s \\ p \end{Bmatrix} = \begin{Bmatrix} F_S \\ F_A \end{Bmatrix} \tag{2.66}$$

where C is the geometrical coupling matrix, $H(\omega)$ is the indirect BEM influence matrix, F_S and F_A are structural and acoustic load vectors. In fully coupled problems, effect of acoustic loading on structure, F_A, is taken into account. However, if the structural response is not affected significantly from incident sound, F_A can be neglected. In the presented case studies weak coupling is assumed and F_A is neglected.

In this study, FEM/BEM coupled method is used in the analysis since boundary element solution is faster for large models and transfer vectors can be implemented in the calculations which will be explained in detail in Chapter 4.

CHAPTER 3

APPLICATION OF STRUCTURAL MODIFICATION WITH ADDITIONAL DEGREES OF FREEDOM TECHNIQUE TO SIMPLE SHAPED STRUCTURES

3.1 Modeling with Finite Elements

In this chapter structural modification technique with additional degrees of freedom, explained in the previous chapter, is studied and different examples are presented. In the case studies the original structure and modifying elements are modeled with finite elements using PATRAN/NASTRAN or ANSYS. Modal analysis of unmodified structure is performed and mode shape and frequency results are obtained. In addition, stiffness and mass matrices of modifying structure are found. Then the results are extracted using the code developed in MATLAB. After applying structural modification technique with additional degrees of freedom, frequency response functions are derived for the modified structure. The frequency response results found from the code are compared with the ones obtained after analyzing the modified structure as a whole in PATRAN/NASTRAN or ANSYS. This procedure can be examined in two sections:

- Finite element modeling and modal analysis

- FRF prediction using structural modification technique

3.2 Finite Element Modeling and Modal Analysis

First, finite element model of the original structure is prepared with the specified geometry, material and element types. Original structure and modifying structure are modeled separately. Modal analysis is performed on the original structure, whereas only mass and stiffness matrices are extracted for the modifying structure.

The following model parameters are needed to construct the finite element model:

- Dimensions and geometry
- Material properties, modulus of elasticity E, density ρ, Poisson's ratio ν
- Element types

After the modal analysis of the original structure, three data sets are found:

- Natural frequencies of the original structure, ω_r
- Mode shapes of the original structure, $\{\phi^r\}$
- Node numbers the of original structure, *node1*

Besides, for the modifying structure it is necessary to extract

- Mass and stiffness matrices, $[\Delta M],[\Delta K]$

- Node numbers of the modifying structure, *node2*

Node numbers of the added structure should be consistent with the original structure node numbers. Then the algorithm finds the coincident nodes, i.e. the nodes shared by both of the structures. Otherwise; the nodes of the original structure where modification is done should be given to the program.

3.2.1 Element Attributions

The finite element modeling is done either by using PATRAN/NASTRAN or by using ANSYS. Element attributions can be different for the two programs. CQUAD4 or CQUADR is used when modeling plate like structures in PATRAN. Instead, SHELL63 is used in ANSYS. For beams CBEAM is used in PATRAN and BEAM4 is used in ANSYS.

Mass formulation of finite elements can be selected as either lumped mass or coupled mass. Lumped mass matrices contain uncoupled, translational components; coupled mass matrices contain translational components with coupling between the other components of mass. In both of the computer programs, coupled mass option is selected.

In finite element programs, condensation techniques are used to reduce degrees of freedom since computing eigenvalues and eigenvectors of systems with many degrees of freedom can be difficult. For instance, in Guyan reduction algorithm [45], mass matrix is condensed to decrease degrees of freedom. The eigenvalue equation is partitioned as

$$\left[\begin{bmatrix} K_{mm} & K_{ms} \\ K_{sm} & K_{ss} \end{bmatrix} - \lambda \begin{bmatrix} M_{mm} & M_{ms} \\ M_{sm} & M_{ss} \end{bmatrix}\right] \begin{Bmatrix} U_m \\ U_s \end{Bmatrix} = \begin{Bmatrix} 0 \\ 0 \end{Bmatrix} \tag{3.1}$$

where m represents master degrees of freedom, and s represents slave degrees of freedom. Assuming the inertia forces of slave degrees of freedom are less important than the elastic forces of master degrees of freedom, only M_{mm} terms are retained in the mass matrix. The other elements of the mass matrix are taken to be zero. On the other hand, no change is made in the stiffness matrix.

In the results of NASTRAN analysis the number of modes and natural frequencies for any element is equal to the number of degrees of freedom associated with mass, i.e. master degrees of freedom. CQUAD4 has only translational terms in the mass matrix element for both lumped and coupled formulations. CQUADR has translational terms and rotational terms associated only to rotational degrees of freedom in the direction normal to the plane of element. However the CBEAM elements contain both translational and rotational masses for coupled formulations.

Shell63 element in ANSYS is an elastic shell element which has four nodes and six degrees of freedom at each node. It has both bending and membrane capabilities. Master degrees of freedom in mass matrix do not contain the degree of freedom in the direction normal to the plane of the element. Beams are modeled with Beam4 element which is a uniaxial element with tension, compression, torsion, and bending capabilities. It has 2 nodes at each element and six degrees of freedom at each node, all of which are master degrees of freedom.

In NASTRAN/PATRAN studies, mass and stiffness matrices of added, i.e. modifying elements are extracted by using *"param ,extout ,dmigpch"* command in the .bdf file. The modified .bdf file is solved by NASTRAN and the resulting .pch file contains mass and stiffness information.

Mass and stiffness matrices of the modifying elements are extracted by substructure analysis using *SEOPT, Sename, 2* option in ANSYS studies.

3.3 Prediction of Frequency Response Functions of the Modified Model

The code developed for structural modification with additional degrees of freedom is prepared in MATLAB. The structural modification method requires FRFs of the original model, dynamic stiffness of the modifying structure and nodal information of both models. Modal analysis of the original structure is performed using a finite element analysis software. Mass and stiffness matrices of added modifications are also extracted using the finite element analysis software. The modal analysis results of original structure, mass and stiffness matrices of modifying structure, node numbers and coordinates are imported by the code.

The code uses the modal analysis results, ω_r and $\{\phi^r\}$ to find FRF of the original structure by using

$$\alpha_{ij} = \sum_{r=1}^{n} \frac{\{\phi_i^r\}\{\phi_j^r\}}{\omega_r^2 - \omega^2 + i\gamma_r\omega_r^2} \tag{3.2}$$

where $\{\phi^r\}$ and ω_r are the *r'*th mode mode shape and the natural frequency, respectively. ω is the circular frequency at which the FRF is calculated, γ_r is the rth structural damping ratio.

If there is damping in the modifying structure, dynamic stiffness matrix of the modifying structure, assuming proportional damping, is calculated as

$$[D] = [\Delta K](1 + i\gamma_s) - \omega^2 [\Delta M] \tag{3.3}$$

where γ_s is the structural damping ratio for all modes. Frequency response function can be calculated at any required node. The other nodes are redundant and are not used in calculations. Thus, only selected degrees of freedom of the original structure are considered in the next steps and matrix sizes are reduced considerably. This approach does not introduce any error in the results.

Data sets containing node numbers, *node*1 and *node*2 are extracted from result files and they are combined and reordered such that new data set contains unmodified nodes in the upper part. Then intersection nodes, and finally nodes belonging only to modifying structure appear in the file.

Receptance matrix α_{ij} is partitioned according to equation (2.15). Dynamic stiffness matrix is calculated using equation (3.3). Receptance matrix of the modified structure is obtained by the modification method explained in Chapter 2.

3.4 Case Studies

In the following case studies structural modification technique with additional degrees of freedom to find the FRF after modification is applied. In order to verify the predicted FRFs, modal analysis is also performed on the modified structure. Using the frequency and mode shape results, receptances are calculated using equation (3.2) and they are taken as references to compare modification results.

3.4.1 Case Study 1 - Beam to Beam

In this example, a beam is modified with another beam attached to one end. PATRAN/NASTRAN is used to model the beams. Original structure is 300 mm long, steel, cantilever beam. It has a rectangular solid cross-section with 4 mm width and 3 mm height. CBEAM elements are used to model the beams. Original beam, added beam and modified beam are shown in Figure 3.1, Figure 3.2, Figure 3.3, respectively.

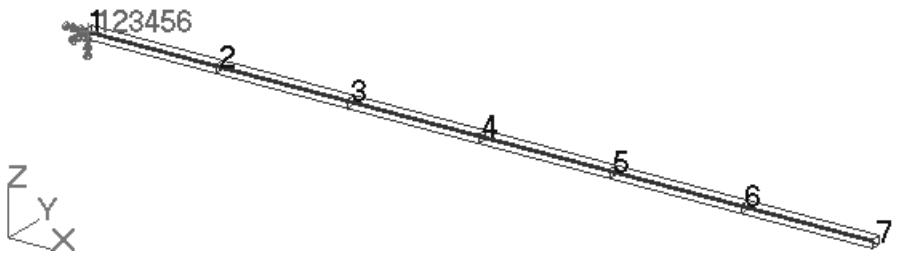

Figure 3.1 Mesh of the original beam

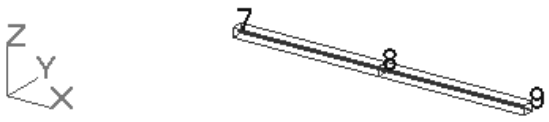

Figure 3.2 Mesh of the added beam

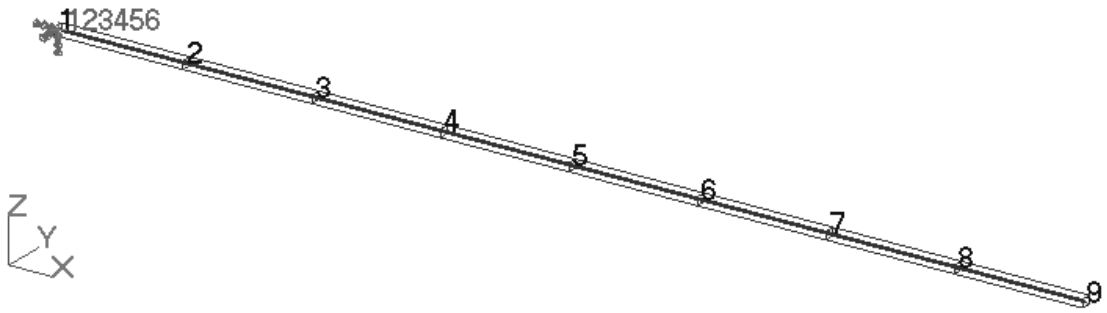

Figure 3.3 Mesh of the modified beam

Elements of both original and added beams are 50 mm long. Two beams are connected at node 7. Original beam has 7 nodes and 36 degrees of freedom since one end is clamped. Added beam has 18 degrees of freedom; therefore

size of its mass and stiffness matrices is 18X18. Modified beam model has 48 degrees of freedom. Details of the model for the first case study are given in Table 3.1.

Table 3.1 Details of the beam-beam modification model

	Original Structure	**Added Structure**
Modulus of elasticity E [GPa]	200	200
Density ρ_S [kg/m³]	7850	7850
Poisson's ratio ν	0.3	0.3
Length [mm]	300	100
Width [mm]	4	4
Height [mm]	3	3
Element type	CBEAM	CBEAM
Number of elements	6	2
Number of nodes	7	3
Degrees of freedom	36	18

In the analysis, structural damping with damping ratio of 0.01 is used in order to compare receptance magnitudes at resonance.

Receptances of the modified beam are obtained also by PATRAN/NASTRAN and the structural modification technique results are compared with them. Since they are taken as reference, all the modes are used to calculate the FRFs. Moreover, in this case study, the effect of truncation is investigated. Point receptance of the modified structure for node 1 in translational z direction between 0-500 Hz is calculated using 10 modes, 20 modes, 25

modes, 28 modes and all modes (36 modes), respectively. Frequency increment is taken as 1 Hz. In Figure 3.4, results of the structural modification technique are shown when 10, 20 or 25 modes of the original beam are used in calculations. It is obvious that the more truncation, the worse the results are.

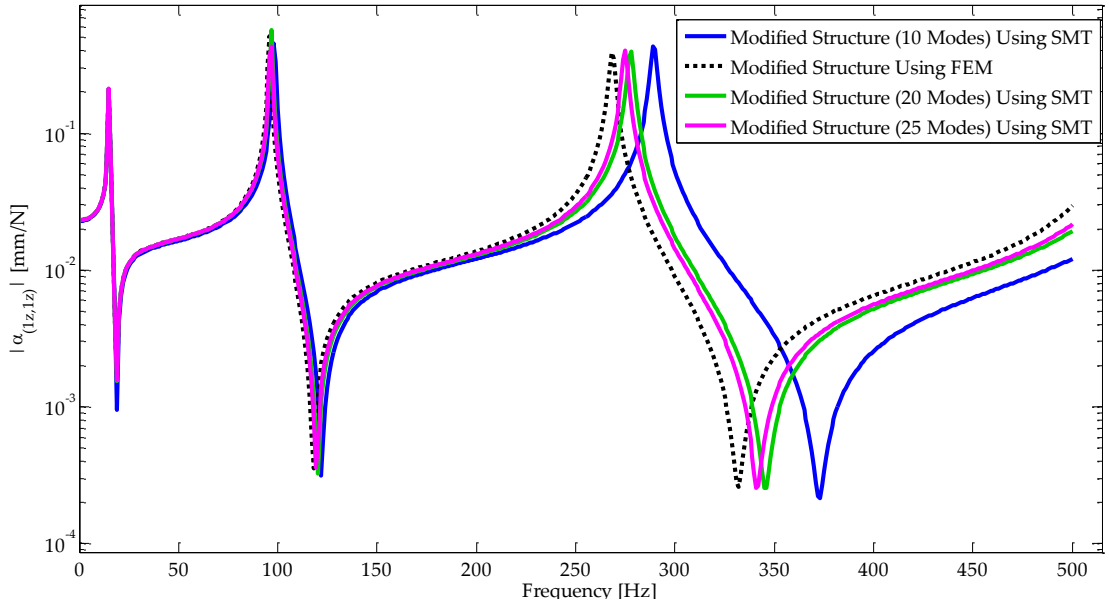

Figure 3.4 Comparison of FRF results for beam-beam modification when some modes are truncated

In Figure 3.5, original beam receptances, modified beam receptances found by modification method are presented. FRFs of the original structure are calculated by using 28 modes and the results are found to be consistent with the ones calculated with PATRAN/NASTRAN. In Figure 3.6, results of the modification when all the modes are used to calculate receptance are presented.

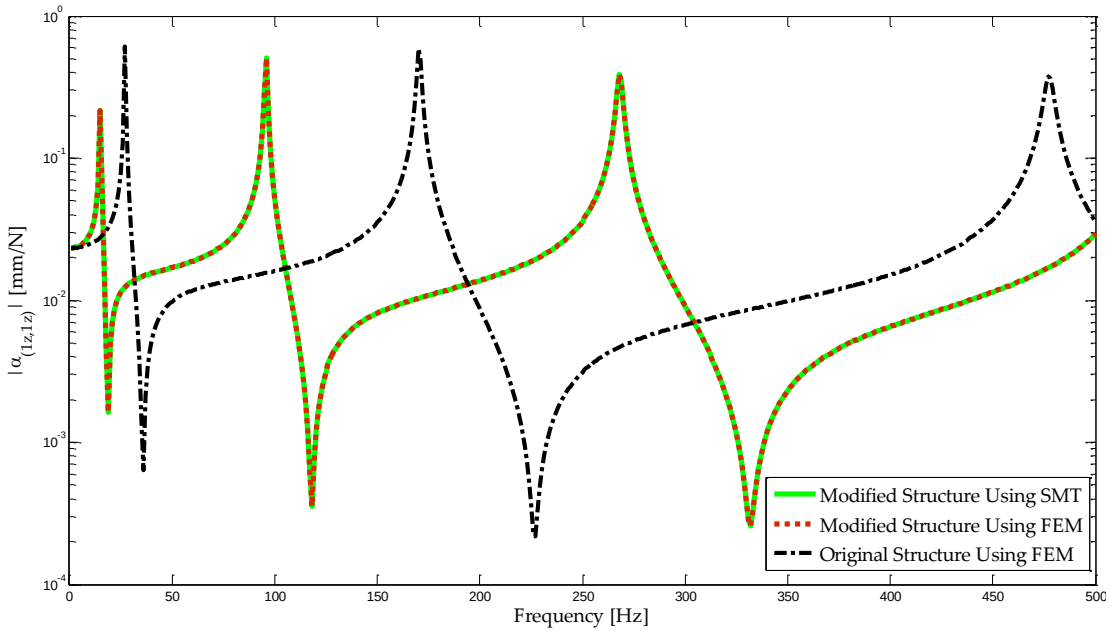

Figure 3.5 Comparison of FRF results of beam-beam modification when the first 28 modes are considered

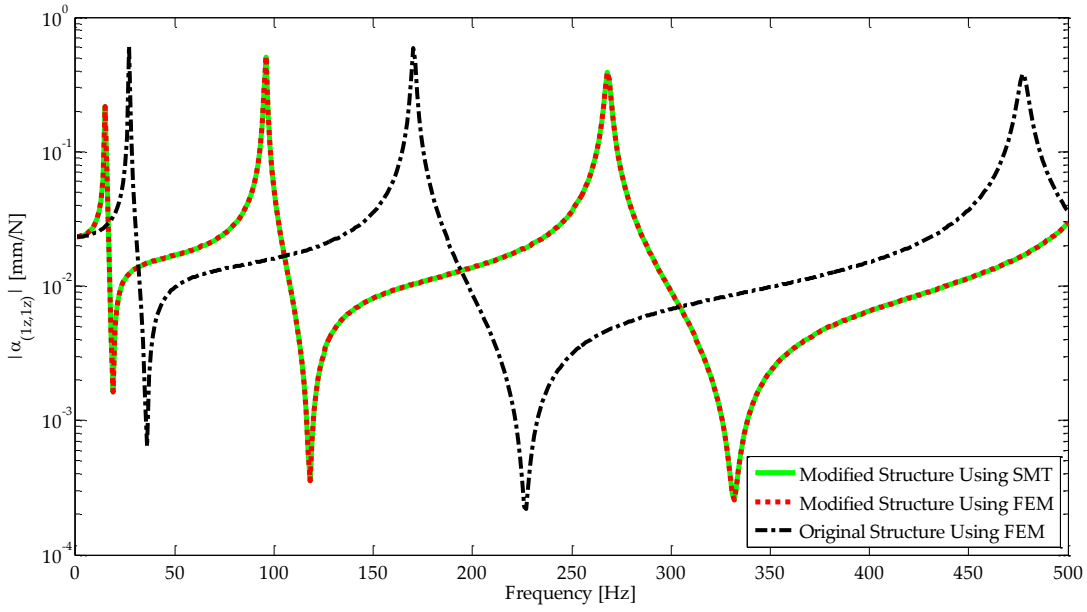

Figure 3.6 Comparison of FRF results of beam-beam modification when all the modes are considered

For this case study, it can be concluded that calculating receptances using only 20, 25 or 28 modes are sufficient to obtain good predictions for the interested frequencies. Effect of truncation should be investigated considering frequency range of interest and computation time.

3.4.2 Case Study 2 - Plate to Plate

In this part, plates are modified with additional plates. In the example of side by side configuration, modifying plate is attached to one end of the original plate. On the other hand, modifying plate is attached onto the original plate for transverse configuration. Plates are modeled with shell elements in all cases.

3.4.2.1 Side by Side Configuration

In this case study, it is aimed to compare results obtained by using the modification technique with the results obtained from two different finite element modeling software and also with analytical results.

Analytically, the natural frequencies of a free-free rectangular plate can be found by using the formula [46]

$$f_{ij} = \frac{\lambda_{ij}^2}{2\pi a^2}\left[\frac{Eh^3}{12\rho_S h(1-\nu^2)}\right],\ \ i=1,2,3\ldots,\ \ j=1,2,3\ldots \tag{3.4}$$

where a is the length of the plate, h is the thickness of the plate, i is the number of half waves in mode shape along horizontal axis, j is the number

of half waves in mode shape along vertical axis, ρ_S is the density, E is the modulus of elasticity, ν is the Poisson's ratio. For free-free square plate, dimensionless frequency parameter, λ_{ij}^2, for the first six modes are given in Table 3.2.

Table 3.2 Dimensionless frequency parameter, λ_{ij}^2 , for free-free square plates [46]

Mode 1	Mode 2	Mode 3	Mode 4	Mode 5	Mode 6
13.49	19.79	24.43	35.02	35.02	61.53

Free-free 200X300 mm aluminum plate of 1 mm thickness is modified with 100X300 mm aluminum plate of the same thickness. The details of the original and modified plate models are given in Table 3.3

Table 3.3 Details of the plate-plate modification model

	Original Structure	**Added Structure**
Modulus of elasticity E [GPa]	71	71
Density ρ_S [kg/m³]	2770	2770
Poisson's ratio ν	0.33	0.33
Length [mm]	200	100
Width [mm]	300	300
Thickness [mm]	1	1

3.4.2.1.1 Plates Modeled with CQUADR Elements

Original plate and modifying plate modeled using CQUADR elements in PATRAN/NASTRAN are shown in Figure 3.7. Resulting modified plate is shown in Figure 3.8. Element sizes are 50 mm x 50 mm. Nodes at the interface of the original and modifying plates have the same numbers and they are coincident.

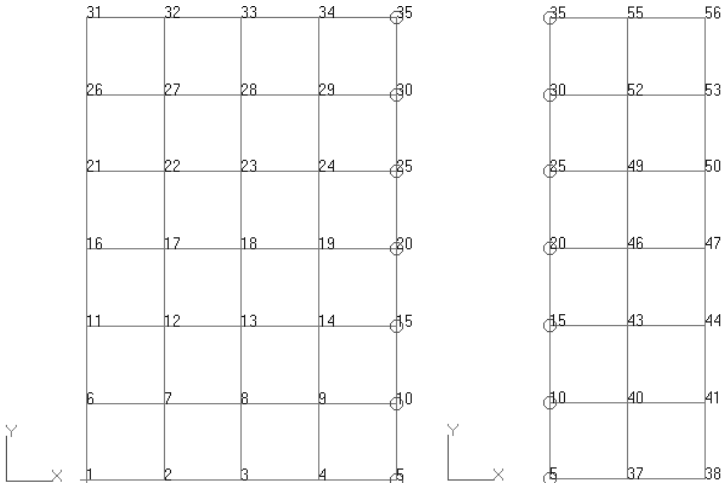

Figure 3.7 Mesh of the original and modifying plates modeled in PATRAN

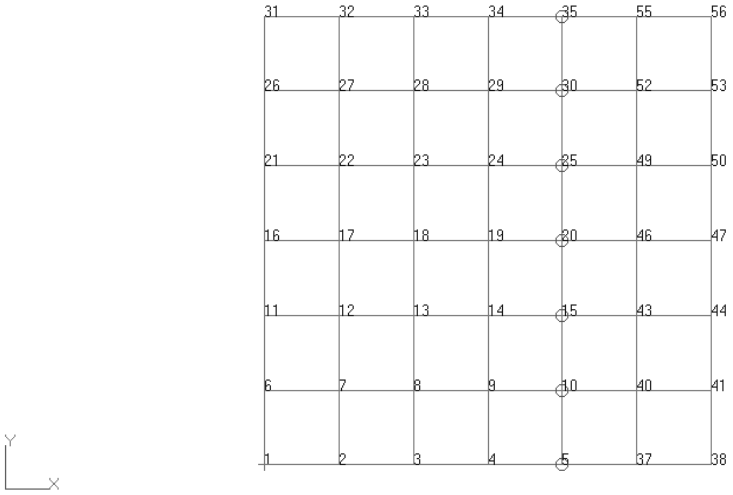

Figure 3.8 Mesh of the modified plate modeled in PATRAN

The details of the finite element model prepared in PATRAN are given in Table 3.4. Original plate with 35 nodes has maximum 136 modes and all of the modes are used to calculate the original plate's receptance. Added plate has 21 nodes and 83 degrees of freedom. The assembled plate model has 192 degrees of freedom.

Table 3.4 Finite element model details for plate-plate side by side modification using PATRAN/NASTRAN

	Original Structure	**Added Structure**
Element type	CQUADR	CQUADR
Number of elements	24	12
Number of nodes	35	21
Degrees of freedom	136	83

Point receptances of modified structure for node 1 in translational z direction between 0-500 Hz with 1 Hz frequency increment are calculated using all modes. Structural damping with a loss factor of 0.01 is assumed. The resulting receptances are shown in Figure 3.9. It is seen that although no truncation is made, there are discrepancies between the predicted FRFs and directly calculated FRFs.

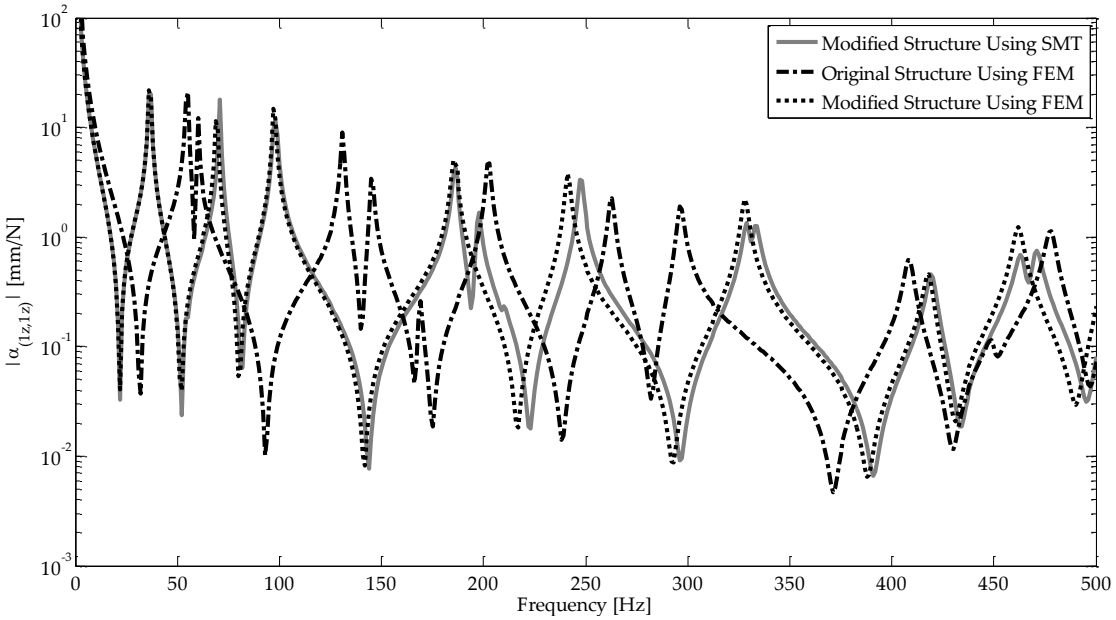

Figure 3.9 Comparison of FRF results for plate-plate modification using CQUADR elements

3.4.2.1.2 Plates Modeled with SHELL63 Elements

The same modification explained in the previous part is also performed using ANSYS. The plates are modeled with Shell63 elements which have 5

degrees of freedom per node as master degrees of freedom. Original and added plates are shown in Figure 3.10 and mesh of the modified plate is shown in Figure 3.11.

Original plate has 24 elements, 35 nodes and 175 degrees of freedom. Modifying plate has 12 elements, 21 nodes and 105 degrees of freedom such that 70 of them are additional degrees of freedom for the original plate. So, the modified plate has 245 degrees of freedom.

Finite element details of this model are those of in Table 3.5. Degrees of freedom for this model are different than the previous one since Shell63 element has 5 master degrees of freedom per node, whereas the number of master degrees of freedom of CQUADR element per node is 4.

Table 3.5 Finite element model details for plate-plate side by side modification using ANSYS

	Original Structure	**Added Structure**
Element type	SHELL63	SHELL63
Number of elements	24	12
Number of nodes	35	21
Degrees of freedom	175	105

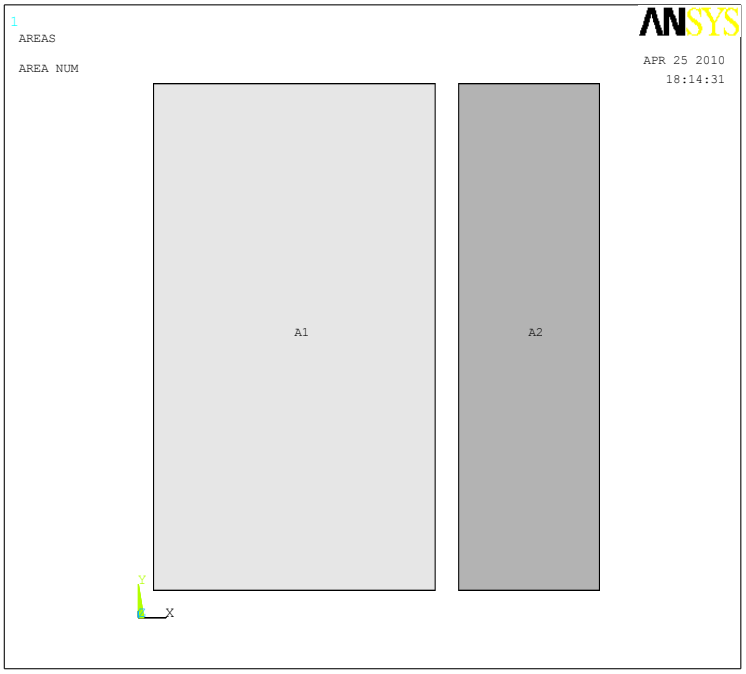

Figure 3.10 Original and modifying plates modeled in ANSYS

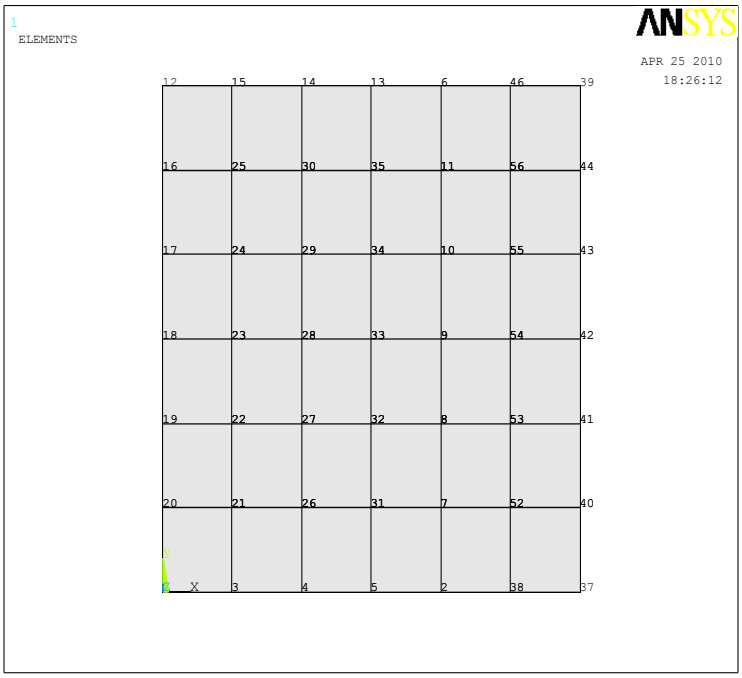

Figure 3.11 Mesh of the modified plate modeled in ANSYS

Similarly, point FRFs of modified plate for node 1 in translational z direction between 0-500 Hz with 1 Hz frequency increment are calculated using all modes. During the FRF calculations, structural damping with a loss factor of 0.01 is assumed. The resulting receptances are shown in Figure 3.12. Unlike the preceding results, Shell63 element gives the same FRFs with the FRFs calculated directly from modal analysis results of the modified plate.

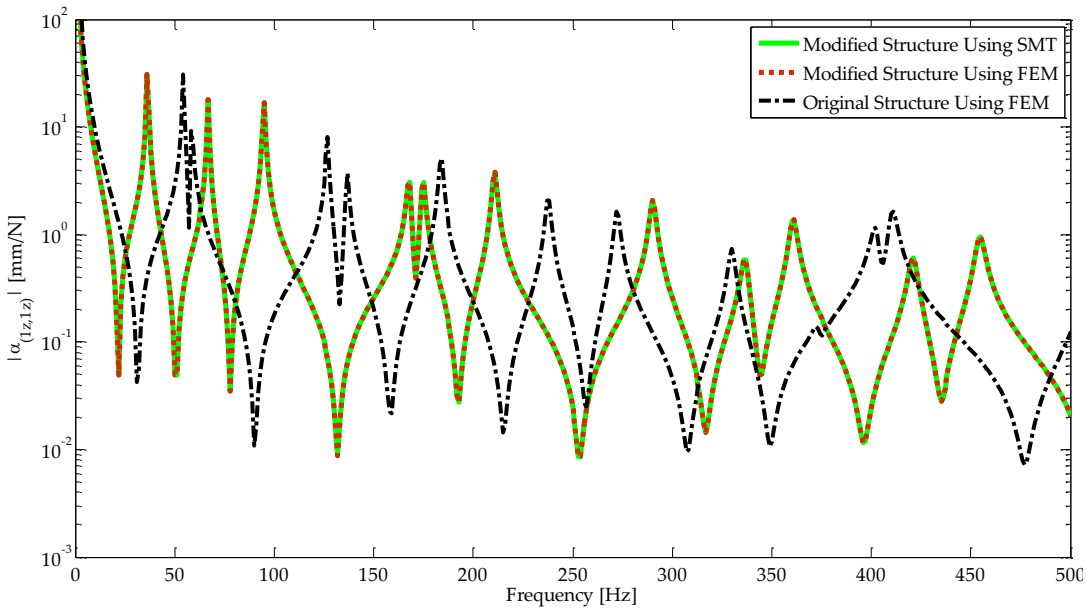

Figure 3.12 Comparison of FRF results for plate-plate modification using SHELL63 elements

3.4.2.1.3 Natural Frequency Comparison of Side by Side Configuration

Exact natural frequencies of the modified free-free aluminum plate, with dimensions 300X300X1 mm are calculated by using equation (3.4). Moreover, natural frequencies of the same plate are calculated by modeling the original

plate directly in PATRAN/NASTRAN and using ANSYS. After combining 200X300X1 mm aluminum plate with 100X300X1 mm aluminum plate, the FRFs of the same square plate are obtained by using structural modification method with additional degrees of freedom, employing the results of PATRAN/NASTRAN and ANSYS. The natural frequencies obtained are compared with the exact ones in Table 3.6. Percentage error is defined with respect to the exact natural frequency as follows:

$$\%Error = \frac{Exact - Predicted}{Exact} 100 \tag{3.5}$$

Table 3.6 Natural Frequencies of 300mm free-free square aluminum plate

Method			**Natural Frequencies [Hz]**					
Exact			36.93	54.18	66.89	95.88	95.88	168.46
CQUADR	**Direct**		36.46	53.97	69.45	97.39	97.39	185.12
		%Error	1.29	0.38	-3.83	-1.57	-1.57	-9.89
	SMT		37	55	69	97	97	185
		%Error	-0.18	-1.51	-3.16	-1.17	-1.17	-9.82
SHELL63	**Direct**		36.29	52.82	67.04	94.83	94.83	167.7
		%Error	1.74	2.51	-0.23	1.10	1.10	0.45
	SMT		36	53	67	95	95	168
		%Error	2.53	2.18	-0.17	0.92	0.92	0.27

It can be concluded that the modification method gives better results for a wide range of frequency if Shell63 element is used to model the plates.

Modifications with CQUADR elements give poor predictions for higher modes. This may be due to the master degrees of freedom in the mass matrices of the elements.

3.4.2.2 Transverse Configuration

The original plate used in this part is the square 1 mm thick aluminum plate with 300 mm edge length. It is meshed with Shell63 elements with 50 mm global edge length. A narrower plate with 3 mm thickness is placed on top of the original plate and its mesh is coincident with the mesh of the original plate. The original plate and the added plate are shown in Figure 3.13. Nodes and elements of the modified plate are illustrated in Figure 3.14.

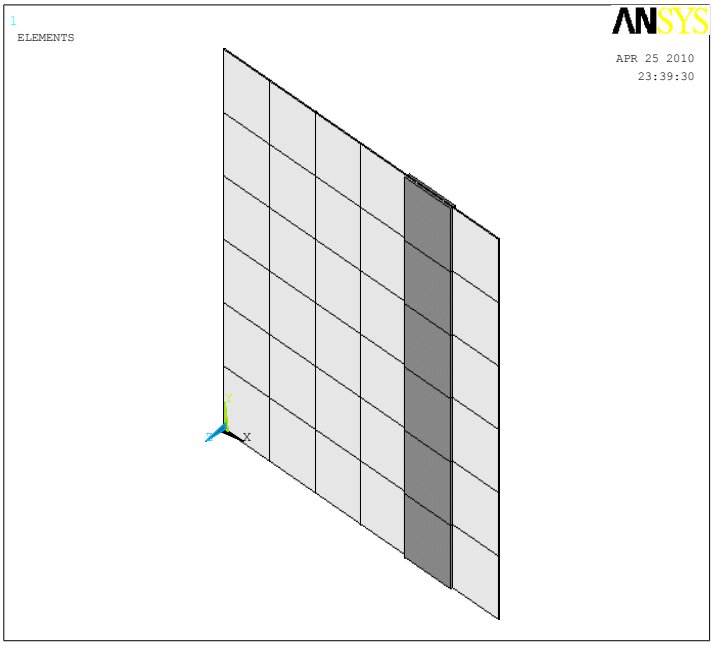

Figure 3.13 Mesh of the original and modifying plates

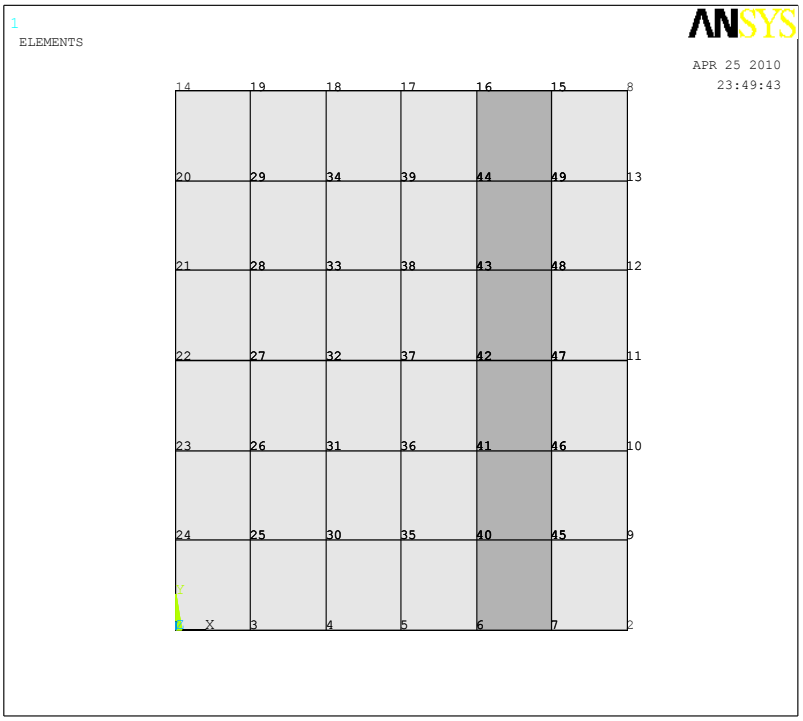

Figure 3.14 Mesh of the modified plate

Original plate has 36 elements, 49 nodes and 245 degrees of freedom. Added plate has 6 elements, 14 nodes and 70 degrees of freedom. The original and modifying plates are connected through 14 nodes having the same numbers. The properties and details of the finite element model are tabulated in Table 3.7. The modified plate has 245 degrees of freedom since the added plate does not impose additional degree of freedom to the original model.

FRFs of the modified plate of node 1 in z direction which is at the bottom left corner is found by using structural modification method. FRFs of the same degrees of freedom in unmodified and modified plate are also found by using the modal analysis in ANSYS. 1 percent structural damping is assumed in calculating the FRFs. Then, the three FRFs are plotted in Figure 3.15 for 0-

500 Hz frequency range with 1 Hz increment. As can be seen from the figure very good agreement is obtained between the results of the modified system calculated by using structural modification method and by using ANSYS directly for the modified system.

Table 3.7 Details of plate-plate transverse modification model

	Original Structure	**Added Structure**
Modulus of elasticity E [GPa]	71	71
Density ρ_S [kg/m³]	2770	2770
Poisson's ratio ν	0.33	0.33
Length [mm]	300	50
Width [mm]	300	300
Thickness [mm]	1	3
Element type	SHELL63	SHELL63
Number of elements	36	6
Number of nodes	49	14
Degrees of freedom	245	70

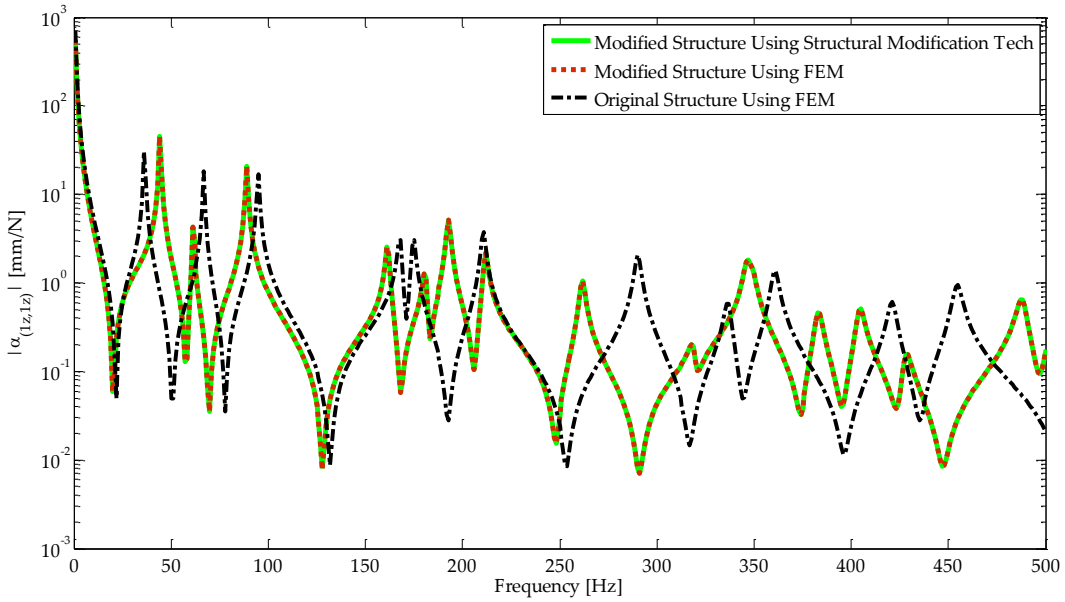

Figure 3.15 Comparison of FRF results for plate-plate transverse modification using SHELL63 elements

3.4.3 Case Study 3 - Beam to Plate

This example includes modification of a free-free square plate with a rectangular cross-section beam. Plate is 300X300X1 mm and beam is 5X300X3 mm. The modified system is shown in Figure 3.16. The plate is modeled with Shell63 elements and it has 36 elements, 49 nodes and 245 degrees of freedom. The beam is meshed with Beam4 elements and it has 6 elements, 7 nodes and 42 degrees of freedom. The resulting modified plate will have 252 degrees of freedom. Additional 7 degrees of freedom come from the beam's degrees of freedom in rotational z direction. Mesh of the modified plate is given in Figure 3.17. Beam4 elements cannot be illustrated in 3D so they are not visible in the figure. They are defined at nodes 6, 16, 40, 41, 42, 43 and 44. The details of the original and modifying structure are given in Table 3.8.

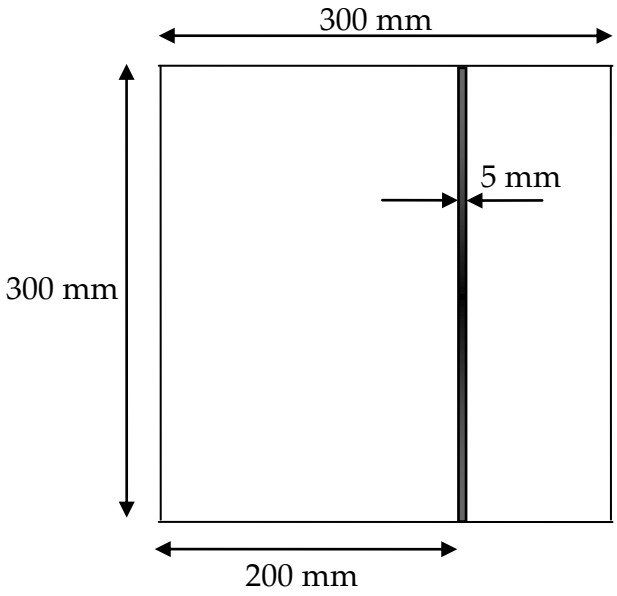

Figure 3.16 Lines of original plate and added beam

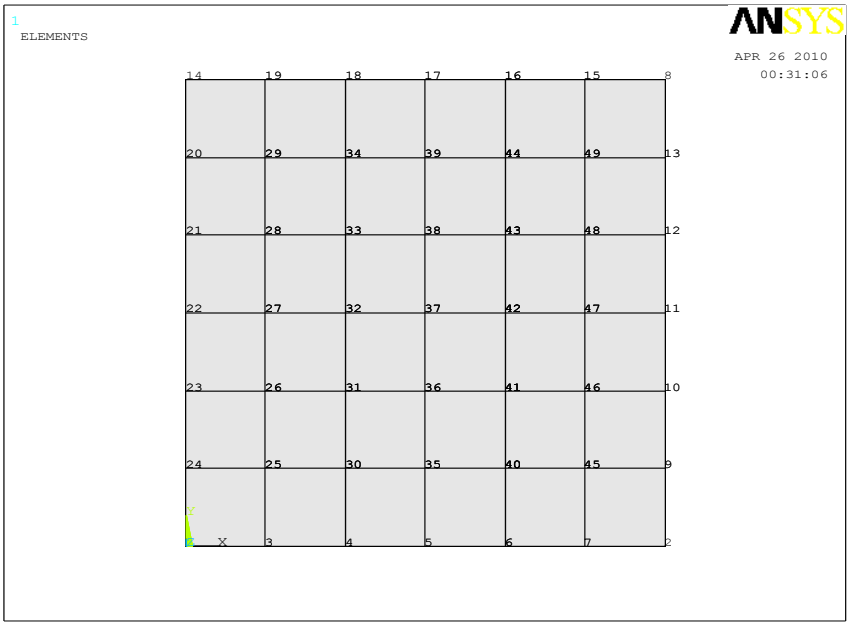

Figure 3.17 Mesh of the modified plate and beam

Table 3.8 Details of beam-plate modification model

	Original Structure	**Added Structure**
Modulus of elasticity E [GPa]	71	71
Density ρ_S [kg/m³]	2770	2770
Poisson's ratio ν	0.33	0.33
Length [mm]	300	300
Width [mm]	300	5
Thickness [mm]	1	3
Element type	SHELL63	BEAM4
Number of elements	36	6
Number of nodes	49	7
Degrees of freedom	245	42

FRFs of modified plate at node 1 in z direction are found using structural modification method. FRFs of the same degree of freedom are also found for the unmodified plate, and then for the modified plate by directly using ANSYS for the modified plate. 1 percent structural damping is assumed in calculating FRFs. Then, the three FRFs are plotted in Figure 3.18 for 0-500 Hz frequency range with 1 Hz increment. As can be seen from the Figure 3.18 very good agreement is obtained between the results of the modified plate calculated by using structural modification method and by using ANSYS directly for the modified plate.

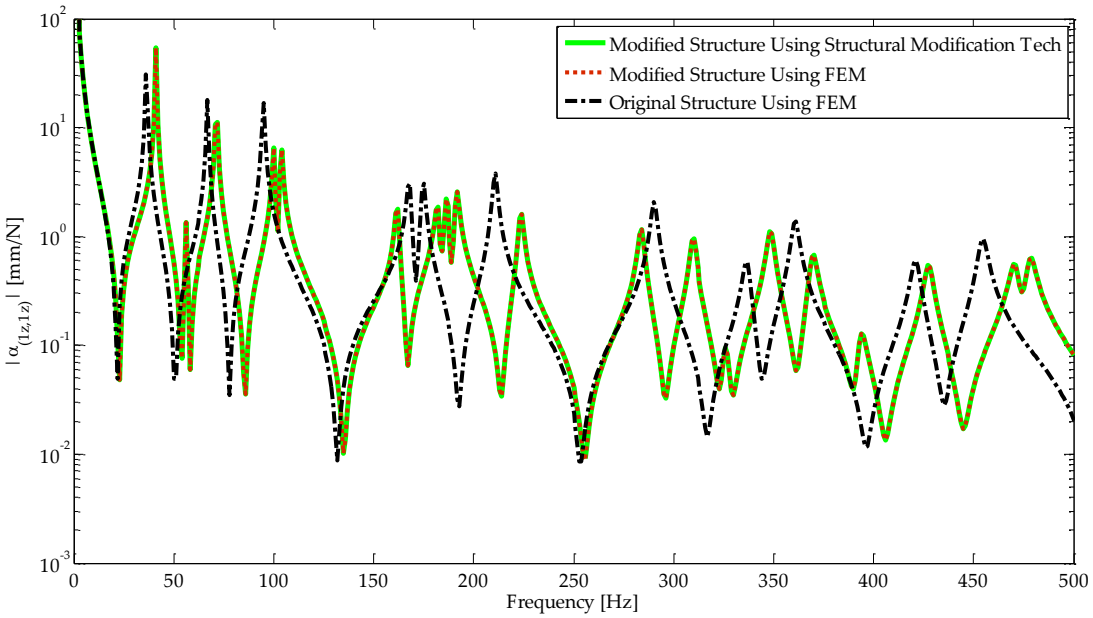

Figure 3.18 Comparison of FRF results for beam-plate modification using BEAM4 and SHELL63 elements

CHAPTER 4

VIBRO-ACOUSTIC ANALYSIS FOR ENCLOSED STRUCTURES

4.1 Modeling of the Acoustic Cavity with Boundary Elements

In this chapter, acoustic analysis of interior domains with boundary element method is studied and case studies are presented. LMS Virtual Lab is used in the analysis. As a first step in the direct analysis (standard) procedure of FEM/BEM coupling, finite element modeling and the modal analysis of structure is performed using finite element software (ANSYS or PATRAN/NASTRAN). Then, the model and the modal analysis results are imported to the LMS Virtual Lab. Based on the finite element model of the structure; acoustic cavity mesh is generated either by using finite elements or by using boundary elements. In this study, acoustic cavity is meshed with 2D boundary elements. In the analysis stage, output points are defined inside the cavity.

In 2D cavity mesh generation step, the mesh size is important. The maximum frequency of interest depends on the size of the elements. As a rule of thumb, one wavelength is composed of six elements [47]. For instance, edge length of an element should be maximum 283 mm to obtain reliable results up to 200 Hz for acoustic analysis.

Two analysis approaches can be used in vibro-acoustic analysis; modal acoustic transfer vector (MATV) and acoustic transfer vector (ATV) approaches. This standard FEM/BEM analysis procedure is illustrated in Figure 4.1. With the use of one of these transfer vectors, sound pressure level can be obtained at any predefined output point. If the transfer vectors are not implemented, the system of equations should be solved each time the structure response changes.

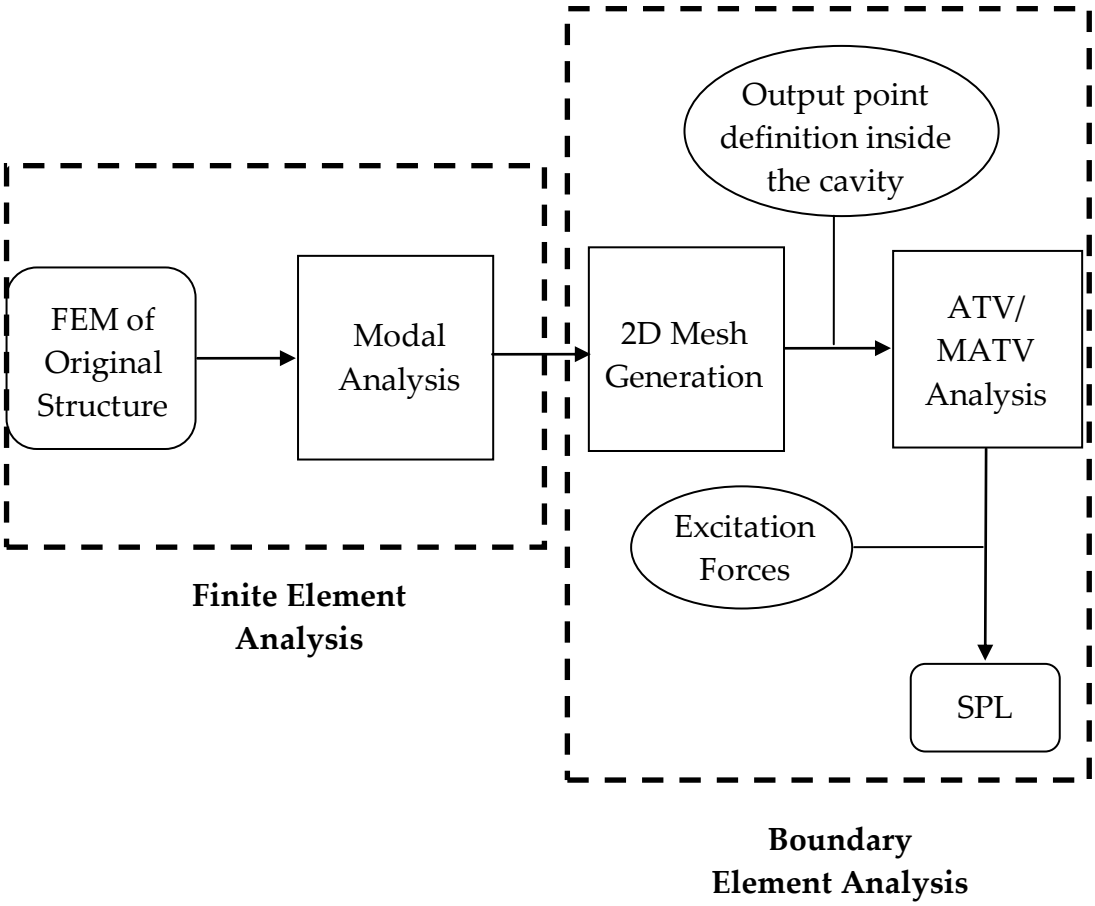

Figure 4.1 Flowchart explaining the standard procedure FEM/BEM method

4.2 Acoustic Transfer Vector and Modal Acoustic Transfer Vector

In boundary element analysis of vibrating systems, transfer vectors (ATV and MATV) are calculated in order to avoid reanalyzing the system when the vibration response changes. These transfer functions are obtained between the surface node velocities and acoustic pressures at designated output field points.

4.2.1 Acoustic Transfer Vector

ATV is the transfer function that relates the surface normal velocity to the sound pressure at a specific output field point. It is calculated once for a defined geometry and an output point for a specific frequency range, and then, can be used every time the response of the structure changes. ATV approach can be formulated as

$$p(\omega) = \{ATV(\omega)\}\{u_n(\omega)\} \tag{4.1}$$

where p is the acoustic pressure at the output point, u_n is the structure's surface normal velocity and ω is the circular frequency. Calculation of ATVs does not require structural excitations. Once the ATVs are obtained, acoustic pressure can be evaluated for different structural response cases by just a matrix multiplication. In the standard FEM/BEM analysis procedure, boundary element analysis program used in this study makes the projection of surface velocities automatically and finds surface normal velocity.

ATVs depend on the geometry and properties of acoustic cavity, acoustic treatment, location of the output point and the frequencies of interest.

4.2.2 Modal Acoustic Transfer Vector

Velocity of structure surface can be written as

$$\{u_n(\omega)\} = i\omega[\phi_n]\{\eta(\omega)\} \tag{4.2}$$

where i is the imaginary number, $[\phi_n]$ is the modal matrix and $\{\eta(\omega)\}$ is the vector of modal coordinates. Then, the acoustic pressure can be expressed in terms of modal participation vectors as

$$p(\omega) = \{MATV(\omega)\}\{\eta(\omega)\} \tag{4.3}$$

MATVs are expressed in modal coordinates and they depend on structural modes. It indicates the contribution of each structural mode to the sound pressure at the output points. If the structure is modified, MATVs should be recalculated. This transfer vector approach is not suitable for structural modification studies. If an optimization process is aimed, ATV method is more suitable.

4.3 Case Studies

In this part vibro-acoustic analysis of a rectangular structure is performed. Dimensions of the structure in the presented case studies are suited for a truck with a compartment. The outer panels of the structure are rigid and the

mid panel is 3 mm thick steel. Mid panel is excited with a unit harmonic force. The sound pressure level at an inside point is obtained following the standard FEM/BEM analysis procedure. Then, the mid panel is modified with a steel strip to change the acoustic response inside the structure. The modified model is analyzed from the beginning as stated in direct analysis procedure.

4.3.1 Case Study 4 - Prediction of SPL of Unmodified Structure

The FEM of the structure is prepared in ANSYS software using Shell63 elements. The details of the model are given in Table 4.1. Modal analysis of the structure is performed for the first 500 modes. The procedure to find sound pressure level inside a closed structure using BEM can be explained as follows:

1. The ANSYS result file ".rst" is imported to the boundary element analysis software LSM Virtual Lab Design.
2. The mode set and the mesh is imported with the appropriate unit system. 0.5 % viscous damping is assumed for the whole structure.
3. Excitation force is defined on the finite element model. The responses as vibration velocity of the structure nodes are obtained.
4. Then, the skin mesh of the finite element model is obtained. This 2D mesh serves as the boundary element mesh for the analysis. In this case, two acoustic cavities are detected, since there is a mid panel, which are illustrated in Figure 4.2.

5. Inside the cavity mesh, field points are defined on which acoustic pressure can be obtained. In this example field point mesh is located at (500, 1000, 800) mm with a 150 mm radius.
6. Material and property of the fluid inside the structure are defined. The BEM details are given in Table 4.2.
7. ATVs between the nodes of boundary elements and the field point nodes are obtained between 1-200 Hz with 1 Hz increment. The calculation time for ATVs is 2158 seconds on a notebook (2 x Intel®Core 1.83 GHz CPU, 1.00 GB RAM). These calculated ATVs can be used for other analysis unless the geometry and properties of the acoustic domain do not change.
8. The vibration velocities are mapped onto the 2D cavity mesh.
9. The output point is defined on the field point mesh at (444.4, 870.6, 746.4) mm. Output point, field point mesh and forcing location are shown on the cavity mesh in Figure 4.3.
10. Finally sound pressure is obtained at the output point. The sound pressures at the field point nodes are calculated in 475 seconds with the use of ATVs on a notebook (2 x Intel®Core 1.83 GHz CPU, 1.00 GB RAM). The resulting A-weighted sound pressure level is shown in Figure 4.4.

Table 4.1 Dimensions and properties of the rectangular structure and stiffener

	Rectangular Box (without Mid-Panel)	**Mid-Panel**	**Modifying strip**
Modulus of elasticity E [GPa]	20000	200	200
Density ρ_S [kg/m³]	7850	7850	7850
Poisson's ratio ν	0.3	0.3	0.3
Panel Thickness, a [mm]	7	3	5
Length [mm]	3260	-	-
Width, b [mm]	1200	1200	20
Height, c [mm]	1400	1400	1400
Element type	Shell63	Shell63	Beam4
Number of elements	856	168	14
Number of nodes	858	195	15
Degrees of freedom	5148	1170	90

Table 4.2 Air properties and BEM details

Density ρ_0 [kg/m³]	1.225
Speed of sound c [m/s]	340
Viscous damping [%]	0.5
Number of elements (2D)	1800
Number of nodes	1804
Element edge length [mm]	100
Max frequency [Hz]	566.667

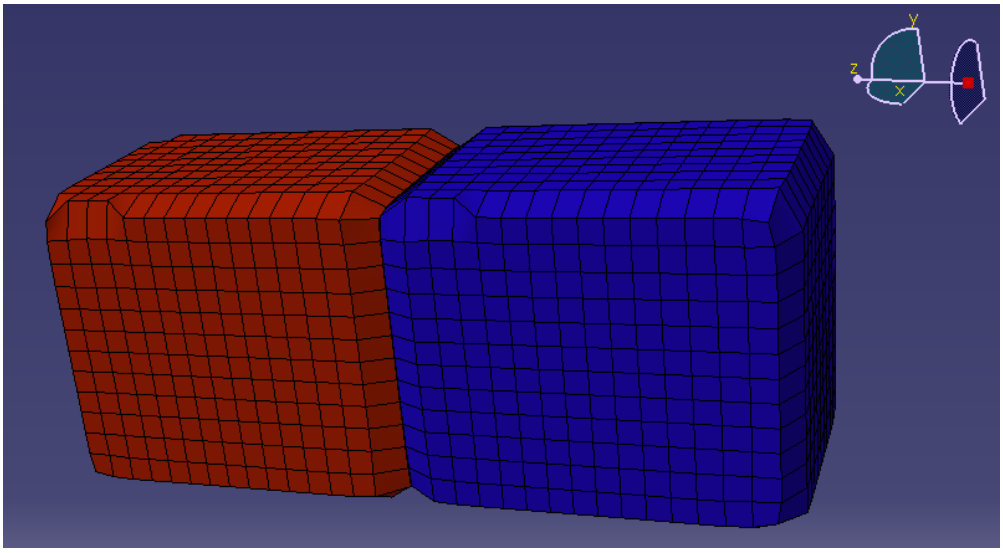

Figure 4.2 Acoustic cavities

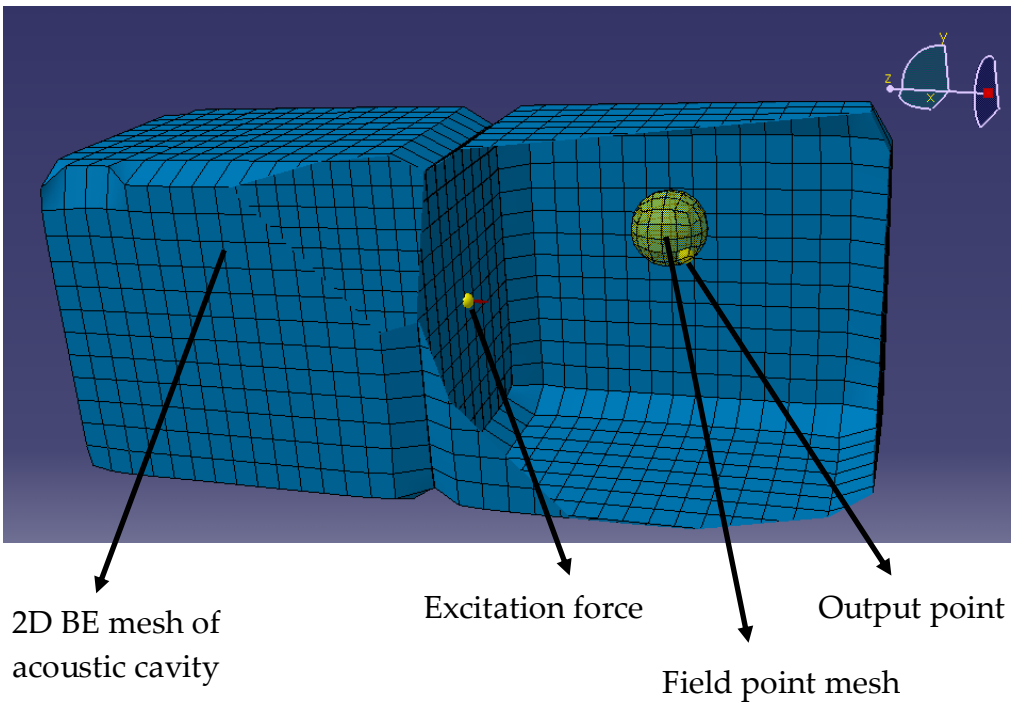

Figure 4.3 2D boundary elements, excitation point, field point mesh and output point

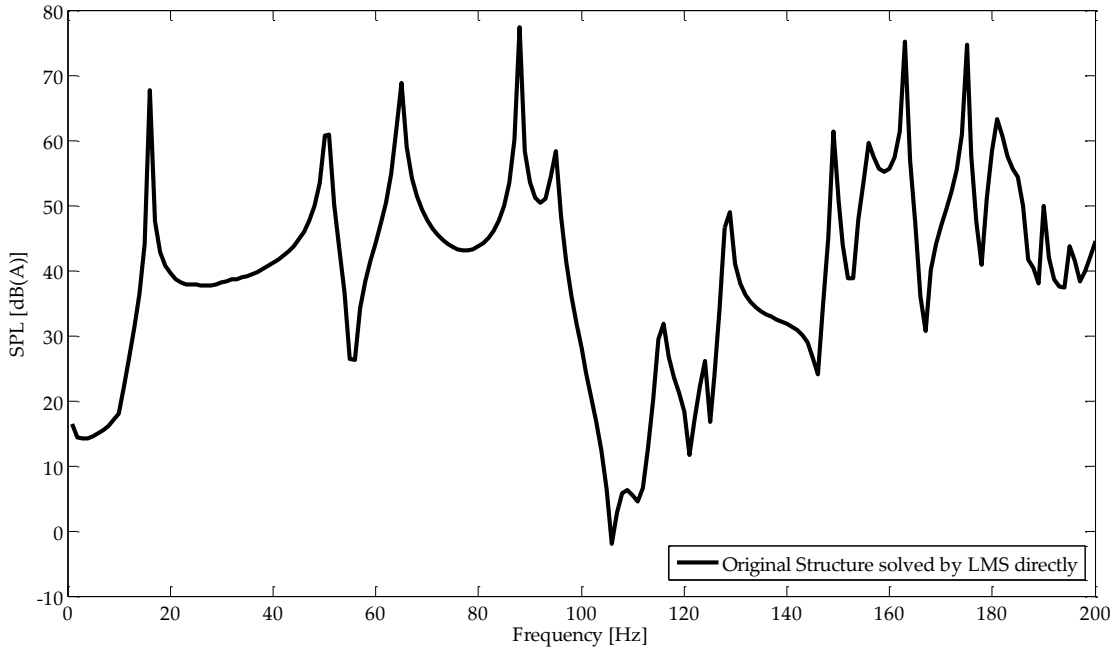

Figure 4.4 SPL(A) for original structure

4.3.2 Case Study 5 - Prediction of SPL of Modified Structure

The mid panel is modified with the steel strip details of which are given in Table 4.1. The added stiffening strip can be seen in Figure 4.5. The same procedure from 1 to 10 is followed again except that the previously calculated ATVs can be reused in this case. The A-weighted sound pressure level at the output point of the modified structure and the original structure are shown in Figure 4.6.

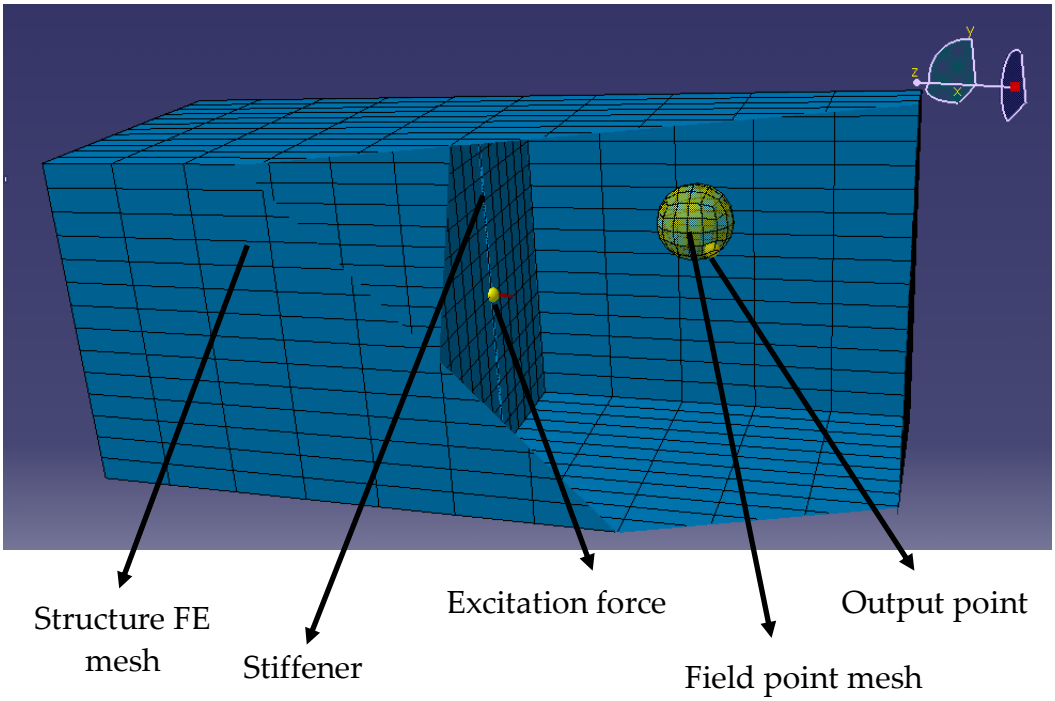

Figure 4.5 Modified structure

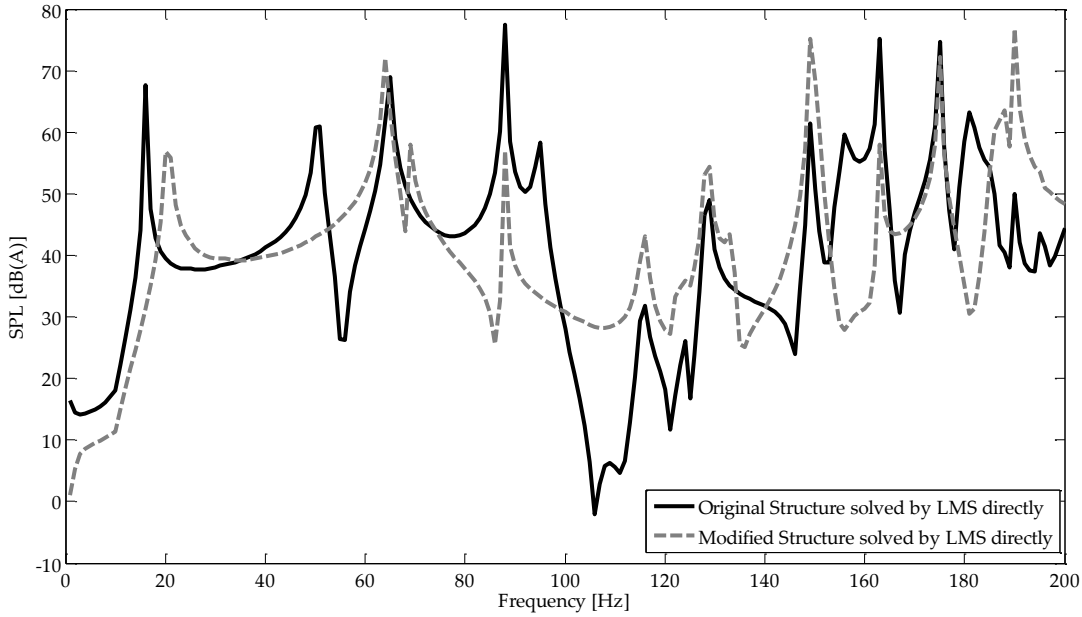

Figure 4.6 SPL(A) comparison for original and modified structures

It is observed that modification on the mid panel caused the first peak to shift to right and the sound pressure is attenuated in the frequency range of 1-100 Hz. At high frequencies the effect is more complicated since there are also increases in the sound pressure levels at some frequency regions (esp. between 100-140 Hz). The modification effects are further investigated in the next chapter using the structural modification method by Özgüven [1].

In this study, effect of acoustic source is also investigated. A monopole is placed in the corner of the acoustic cavity at (100, 100, 100) mm. Acoustic pressure due to a monopole at a distance r in the free field is expressed as

$$p(r,t) = i\rho_0 ck \frac{Q}{4\pi r} e^{i(\omega t - kr)} \tag{4.4}$$

where Q is the monopole strength having the unit of m^3/s.

Monopole can be defined as constant or frequency dependent in LMS Virtual Lab and its unit is kg/s^2 which corresponds to the terms $\rho_0 ckQ$. In the presented case study, monopole strength is defined as 0.01 kg/s^2 constant value. In the solution procedure ATV approach is not used and the solution time for frequencies 1-200 Hz with 1 Hz increment is 1718 seconds on a notebook (2 x Intel®Core 1.83 GHz CPU, 1.00 GB RAM). The results for the same modification problem are shown in Figure 4.7. It is observed that between 100 and 140 Hz modification does not cause a significant increase in the sound pressure levels. Modification effect is as emphasized for 40-60 Hz region, around 80 Hz and 185 Hz.

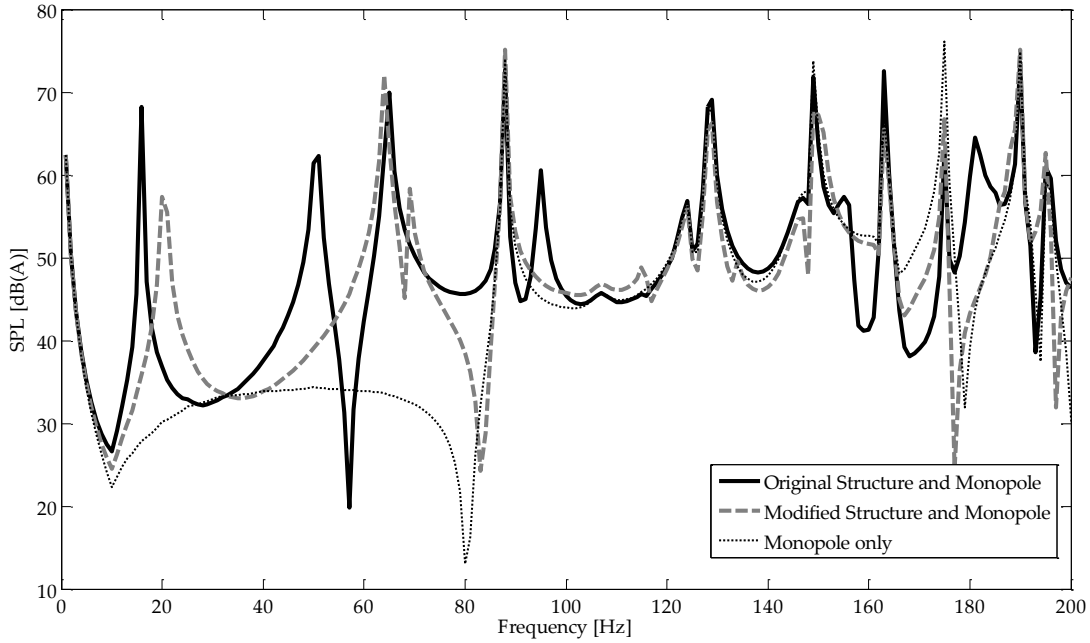

Figure 4.7 SPL(A) comparison for original and modified structures with a monopole inside the cavity

CHAPTER 5

INTEGRATION OF STRUCTURAL MODIFICATION TECHNIQUE WITH THE VIBRO-ACOUSTIC ANALYSIS

5.1 Introduction

In this chapter a rectangular structure which is divided into two parts to represent a truck with a compartment is investigated. The aim is to develop a method to predict changes in acoustic characteristics inside the closed structure due to the modifications made on the structure in a more efficient way. Different configurations and different widths of strips are applied to the flexible wall and sound pressures at an inside location are compared to see the modification effects.

5.2 Description of the Finite Element Model

The structure is a closed rectangular geometry with dimensions 1200x1400x3600 in mm with a panel at the middle which is shown in Figure 5.1 with hiding two outer walls. The outer walls of the structure are modeled as rigid parts by assigning a very high elastic modulus. Mid panel is 3 mm thick steel plate and it behaves like a fully clamped plate since the other walls are rigid. The details of the structure are given in Table 5.1. Modal analysis of the whole model is performed in ANSYS to obtain natural

frequencies and mode shapes. Only flexible part in the structure is the mid panel. So its modal information is extracted from the results of modal analysis. Nodes belonging to the rigid walls are redundant and their modal data are not included in the analysis for this case. The FRFs are calculated using equation (3.2) and 0.01 structural damping is assumed.

The first six modes are rigid body modes of the structure and corresponding natural frequencies are zero. The first 30 non-zero natural frequencies of the structure are given in Table 5.2 , Table 5.3 and Table 5.4 for different element sizes: ES 1, ES 2, and ES 3, respectively. ES 1 corresponds to 200 mm, ES 2 corresponds to 100 mm, and ES 3 corresponds to 50 mm element edge length for mid panel. These frequencies can be compared with the analytical natural frequencies of fully clamped plate since the mid panel behaves like fully clamped plate. The results presented in Table 5.5 illustrate the validity of this assumption. The exact natural frequencies of fully clamped 1200x1400mm steel plate are obtained by using equation (3.4). Dimensionless frequency parameters, λ_{ij}^2 are presented by Leissa [48] and they are given in Table 5.6.

Table 5.1 Dimensions and properties of the rectangular structure

	Rectangular Box (without Mid Panel)	**Mid Panel**
Modulus of elasticity E [GPa]	20000	200
Density ρ_S [kg/m³]	7850	7850
Poisson's ratio ν	0.3	0.3
Panel Thickness [mm]	7	3
Length [mm]	3260	-
Width, b [mm]	1200	1200
Height, c [mm]	1400	1400

Table 5.2 First 30 natural frequencies of the original structure (ES 1)

Modes	**Frequency [Hz]**		**Modes**	**Frequency [Hz]**		**Modes**	**Frequency [Hz]**
1	15.84		**11**	91.87		**21**	147.62
2	28.68		**12**	102.84		**22**	148.27
3	34.61		**13**	111.04		**23**	148.61
4	45.86		**14**	113.91		**24**	152.46
5	49.72		**15**	115.60		**25**	153.30
6	63.92		**16**	121.91		**26**	160.50
7	65.06		**17**	124.76		**27**	164.29
8	73.61		**18**	126.58		**28**	173.74
9	78.20		**19**	138.62		**29**	174.15
10	90.95		**20**	145.93		**30**	176.23

Table 5.3 First 30 natural frequencies of the original structure (ES 2)

Modes	Frequency [Hz]		Modes	Frequency [Hz]		Modes	Frequency [Hz]
1	16.02		**11**	95.13		**21**	153.74
2	29.16		**12**	104.13		**22**	155.85
3	35.11		**13**	114.82		**23**	158.35
4	47.14		**14**	115.53		**24**	158.87
5	50.55		**15**	121.56		**25**	163.77
6	64.79		**16**	121.90		**26**	173.40
7	67.26		**17**	130.51		**27**	174.63
8	75.89		**18**	132.88		**28**	177.54
9	79.31		**19**	138.84		**29**	180.93
10	94.88		**20**	148.94		**30**	185.81

Table 5.4 First 30 natural frequencies of the original structure (ES 3)

Modes	Frequency [Hz]		Modes	Frequency [Hz]		Modes	Frequency [Hz]
1	16.07		**11**	96.34		**21**	154.62
2	29.30		**12**	104.72		**22**	159.07
3	35.27		**13**	116.09		**23**	159.84
4	47.54		**14**	116.25		**24**	161.91
5	50.83		**15**	123.18		**25**	165.57
6	65.12		**16**	123.83		**26**	175.66
7	68.02		**17**	132.26		**27**	176.81
8	76.67		**18**	135.15		**28**	179.74
9	79.79		**19**	140.38		**29**	184.16
10	96.34		**20**	150.67		**30**	187.62

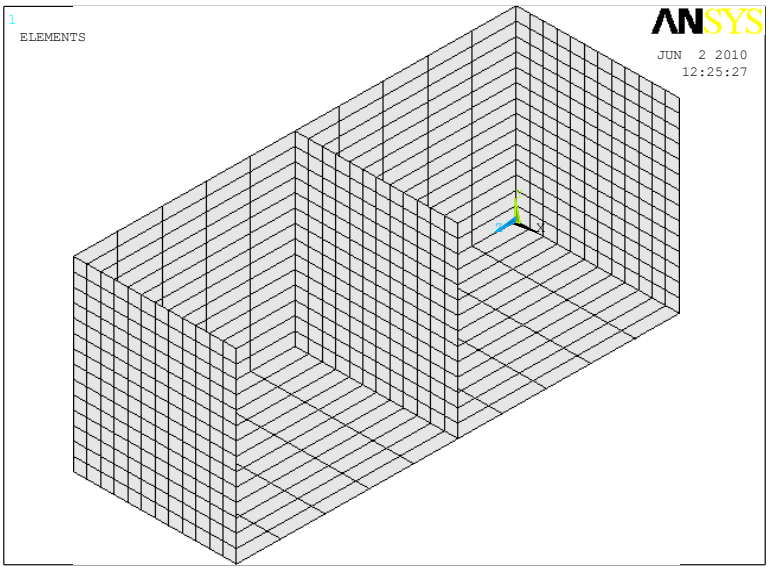

Figure 5.1 FEM of the structure (two walls are hidden)

Table 5.5 Natural frequencies of 1200x1400 mm fully clamped steel plate

Method			**Natural Frequencies [Hz]**								
Exact			15.95	29.47	35.35	47.83	51.14	65.17	68.58	77.10	80.48
FEM	**ES 1**		15.84	28.68	34.61	45.86	49.72	63.92	65.06	73.61	78.20
		% Error	0.69	2.68	2.09	4.12	2.78	1.92	5.13	4.53	2.83
	ES 2		16.02	29.16	35.11	47.14	50.55	64.79	67.26	75.89	79.31
		% Error	-0.44	1.05	0.68	1.44	1.15	0.58	1.92	1.57	1.45
	ES 3		16.07	29.30	35.27	47.54	50.83	65.12	68.02	76.67	79.79
		% Error	-0.75	0.58	0.23	0.61	0.61	0.08	0.82	0.56	0.86

Table 5.6 Dimensionless frequency parameter, λ_{ij}^2 , for 1200x1400 mm (a/b=0.86) fully clamped steel plate [48]

Modes	1	2	3	4	5	6	7	8
λ_{ij}^2	31.4881	58.1954	69.7990	94.4293	100.9822	128.6797	135.4162	158.9113

When Table 5.5 is investigated, it is observed that model with ES 1 which corresponds to 200 mm edge length does not give accurate results; ES 2 and ES 3 give better results. This case can be further investigated by comparing element edge length and bending wave length of the plate. Bending wave length of the plate is given by [49]

$$\lambda_B = \frac{1}{f}\sqrt{2hf\sqrt{\frac{E}{\rho}}} \tag{4.5}$$

where h is the thickness of the plate, f is frequency in Hz, E is modulus of elasticity and ρ is the density. At 200 Hz, bending wave length of the steel plate with the given properties is 389 mm. If one wave is represented by 6 elements, element edge length should be at most 65 mm to have accuracy up to 200 Hz. However, in the case studies, ES 2 is selected to model the mid plate to have small size matrices. It shown in Table 5.3, Table 5.4 ad Table 5.5 that ES 2 and ES 3 give very close results which would cause no significant difference in the analysis results.

5.3 Structural Modification by Adding Stiffeners

The structural modification technique used in this study allows predicting modified system responses without repeating the same modal analysis. Moreover, receptances of the whole structure need not to be calculated in the analysis. Receptances of redundant nodes are not used in the calculations. Due to this reason modal information of nodes only at the mid panel are extracted and used in the structural modification calculations.

In the following case studies, first, the element type to model the structure is examined. Then, the number of modes to be included in the structural modification analysis is decided. This step is important since the structural modification may yield erroneous results if sufficient number of modes is not included. Mesh size of the model is also investigated. Two different mesh sizes are compared to see the differences in the receptances. In the last case study, strips of different configurations and different widths are applied on the mid panel to change the vibration response. Effects of these changes on sound pressure levels are investigated.

5.3.1 Case Study 6 – Element Type Comparison

In the first approach, the original structure is modeled with Solid45 elements in ANSYS element library. In the second approach, Shell63 elements in ANSYS element library are used and the resulting model is shown in Figure 5.1. For the two models, element sizes are kept equal. Modal analysis is performed for the first 500 modes. Receptances of the original box is calculated using equation (3.2). Structural damping with a loss factor of 0.01

is assumed in the FRF calculations. The receptances at the mid node (node 982) of mid panel are plotted in Figure 5.2. The frequency increment in the calculations is taken as 1 Hz.

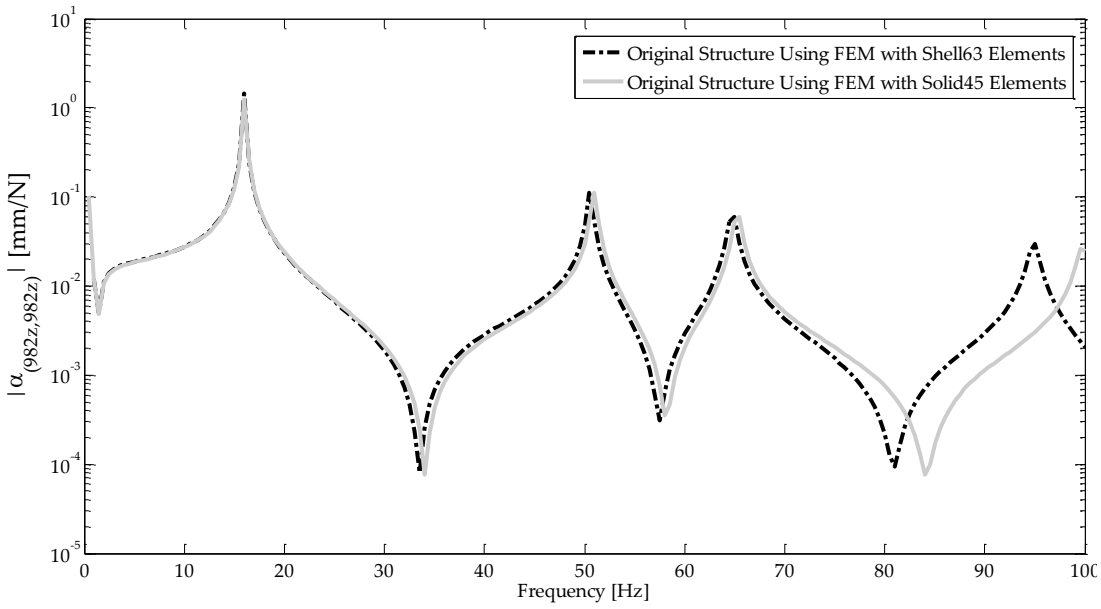

Figure 5.2 Comparison of FRF results of original structure modeled with Solid45 and SHELL63 elements

It is seen in Figure 5.2 that at low frequencies Shell63 and Solid45 element types give the same results, but at high frequencies there exists some discrepancy. In this study, shell63 elements will be used to model the structure panels since they are suitable to represent plate structures allowing high length/thickness aspect ratio.

5.3.2 Case Study 7 – Truncation of Modes

In this part the structure is modified with 200x800x5 mm steel strip which is shown in Figure 5.3 with dark gray elements. The wall thicknesses are exaggerated in this figure to show the relative thicknesses of panels. The FEM details of this case are tabulated in Table 5.7. Mode truncation effect which was presented in the previous section is examined for this structure. Modal information of the first 1000 modes of original structure is extracted from modal analysis results. Dynamic stiffness matrix of the modifying plate is obtained using the mass and stiffness matrices extracted from ANSYS. Then the structural modification technique is applied by using 500 and then 1000 modes. Structural damping with a loss factor of 0.01 is assumed in the calculations.

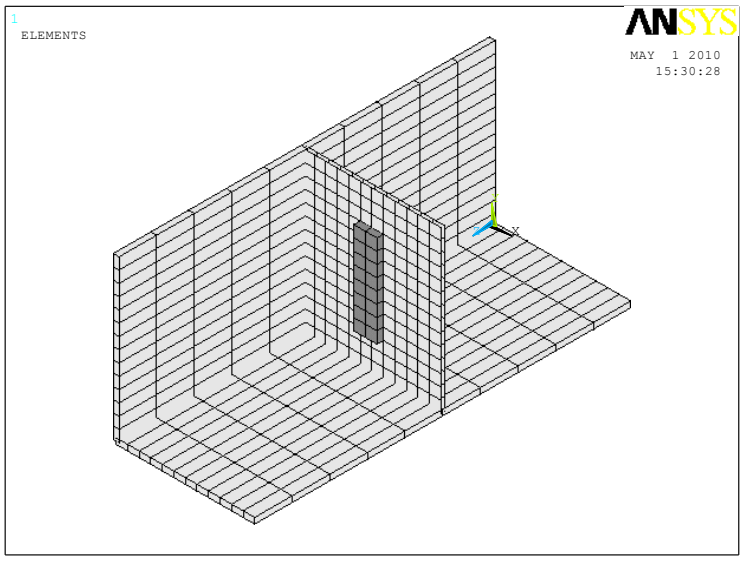

Figure 5.3 FEM of structure and modifying strip (four walls are hidden)

Table 5.7 FEM details for the original structure and the modifying plate

	Rectangular Box (without Mid-Panel)	**Mid-Panel**	**Modifying plate**
Modulus of elasticity E [GPa]	20000	200	200
Density ρ_S [kg/m³]	7850	7850	7850
Poisson's ratio ν	0.3	0.3	0.3
Thickness, a [mm]	-	3	5
Width, b [mm]	-	1200	200
Height, c [mm]	-	1400	800
Element type	Shell63	Shell63	Shell63
Number of elements	856	168	16
Number of nodes	858	195	27
Degrees of freedom	5148	1170	96
Structural Damping [%]	1	1	1

The results of structural modification are shown in Figure 5.4. The plotted FRFs belong to the node in the middle of the mid panel. Modal analysis of the modified structure is also performed and resulting FRF is plotted to compare the modification results. When compared with the original system's FRF, it is seen that the modification on the mid panel changes the response magnitudes and shifts the resonant frequencies. Moreover, when the FRFs of modified panel obtained by using 500 modes and the FRFs obtained directly by ANSYS are compared, there are small discrepancies at higher frequencies. This is due to the truncation of modes. On the other hand, when 1000 modes

are used in structural modification code, the results of direct analysis and structural modification method coincide.

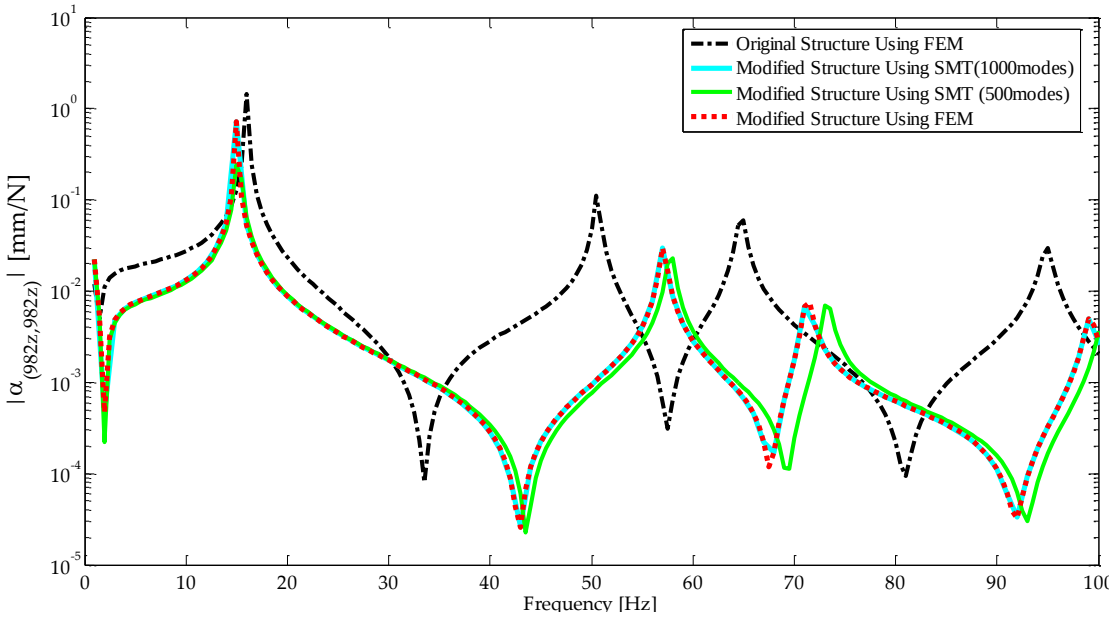

Figure 5.4 Comparison of FRF results of modified structure obtained by taking 500 modes or 1000 modes of original structure

5.3.3 Case Study 8 – Mesh Size Comparison

Mesh size of the model directly affects the time to solve the structural modification problem since the size of matrix to be inverted changes. On the other hand, the mesh of the model should be fine to represent the real situation accurately. The same rectangular cavity presented in the previous case studies 6 and 7 is investigated with different element sizes summarized in Table 5.8 and Table 5.9. The modifying strip is 1400 mm long. It has a

thickness of 5 mm and width of 30 mm. For fine mesh model, the first 1000 modes are used, whereas for coarse mesh model the first 500 modes are used in the calculations. For the coarse mesh case, taking 500 modes is enough since the number of degree of freedom is small. Structural damping with a loss factor of 0.01 is introduced at each case. For both of the cases FRFs are calculated between 0-200 Hz with 1 Hz increment.

Table 5.8 FEM details for model with fine mesh

	Rectangular Box (without Mid-Panel)	**Mid-Panel**	**Modifying Strip**
Modulus of elasticity E [GPa]	20000	200	200
Density ρ_S [kg/m³]	7850	7850	7850
Poisson's ratio ν	0.3	0.3	0.3
Element type	Shell63	Shell63	Beam4
Number of elements	856	168	14
Number of nodes	858	195	15
Degrees of freedom	5148	1170	90

Table 5.9 FEM details for model with coarse mesh

	Rectangular Box (without Mid-Panel)	**Mid-Panel**	**Modifying Strip**
Modulus of elasticity E [GPa]	20000	200	200
Density ρ_S [kg/m³]	7850	7850	7850
Poisson's ratio ν	0.3	0.3	0.3
Element type	Shell63	Shell63	Beam4
Number of elements	344	42	7
Number of nodes	345	56	8
Degrees of freedom	2070	336	48

The point FRF results are plotted in Figure 5.5 for point P at (600, 800, 1630) mm. Mesh size affects the modal analysis results especially at higher frequencies. This effect is more distinct than the effect of truncation of modes. The model with finer mesh can be selected to continue analyzing the vibro-acoustic problem.

As stated before, number of degrees of freedom of the modifying elements determines the computational time of structural modification code. For instance, the elapsed time for only structural modification routine is 396 seconds for fine mesh case and 27 seconds for coarse mesh case on a notebook (2 x Intel®Core 1.83 GHz CPU, 1.00 GB RAM). The number of modified degrees of freedom is doubled and mode number extracted and used in the calculations is doubled. As a result the solution time is increased

by 15 times. The solution time variation due to the number of degrees of freedom of the original model and modifying elements is studied in a previous study by Köksal et al. [32] in detail.

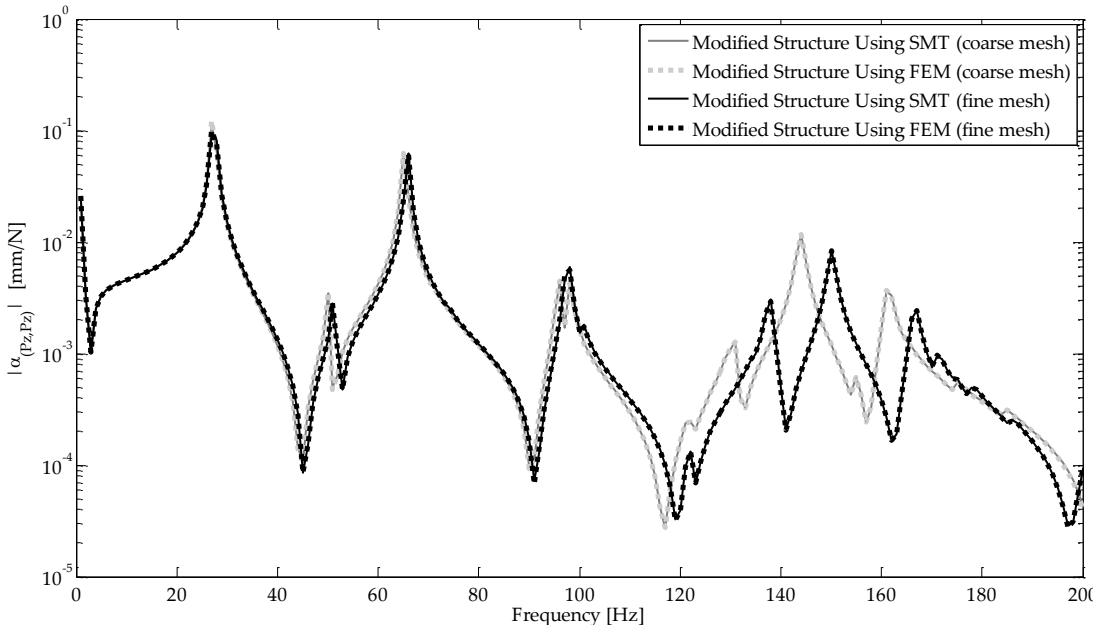

Figure 5.5 Point FRF of point P for two different mesh sizes

5.4 Description of the Boundary Element Model

For the analysis of acoustic domain excited by structure vibration, BEM requires vibration velocity (displacement/acceleration) of the structure in the normal direction as boundary conditions. Solving the Helmholtz integral equation with the boundary conditions, acoustic pressure at a predefined interior (or exterior) point can be obtained.

In BEM procedure, ATV approach is preferred in the scope of this study. ATV can be defined as transfer vector between vibration response of surfaces and acoustic pressure at the desired points. This transfer vector depends on the geometry of acoustic cavity, acoustic treatment and location of output point. ATV results are then used for all modification cases since addition of stiffeners do not change the geometry and the acoustic properties of the 2D cavity model.

5.5 Description of FEM/BEM Method with Structural Modification Technique

In the standard FEM/BEM coupled method used for vibro-acoustic analysis in LMS Virtual Lab program, which is explained in the previous chapter, finite element model and modal data including natural frequencies and mode shapes are imported into the program for every modified system. Excitation force is defined inside the LMS Virtual Lab (or it can be imported as excel file) and the program calculates the vibration velocities using the modal data. These velocities are then used as boundary conditions for the BEM part. So, modal analysis of the system after modification should be performed in ANSYS (or other FEM software), which requires considerable amount of time if the model is very large, and imported to LMS Virtual Lab program. However, in the developed methodology, original system is analyzed in ANSYS only once. Then, the dynamic stiffness of added structure is obtained using ANSYS considering only the added elements. Structural modification technique allows finding the modified system response using original system modal data and dynamic stiffness of the

modifying structure. Imaginary and real components of calculated velocities are then exported to EXCEL files. In other words, the vibration velocities are evaluated outside the LMS Virtual Lab and imported to the program. In this method, LMS Virtual Lab is used only for BEM analysis. Using the previously calculated ATVs, SPL at the predefined output point is obtained. The procedure is illustrated in Figure 5.6.

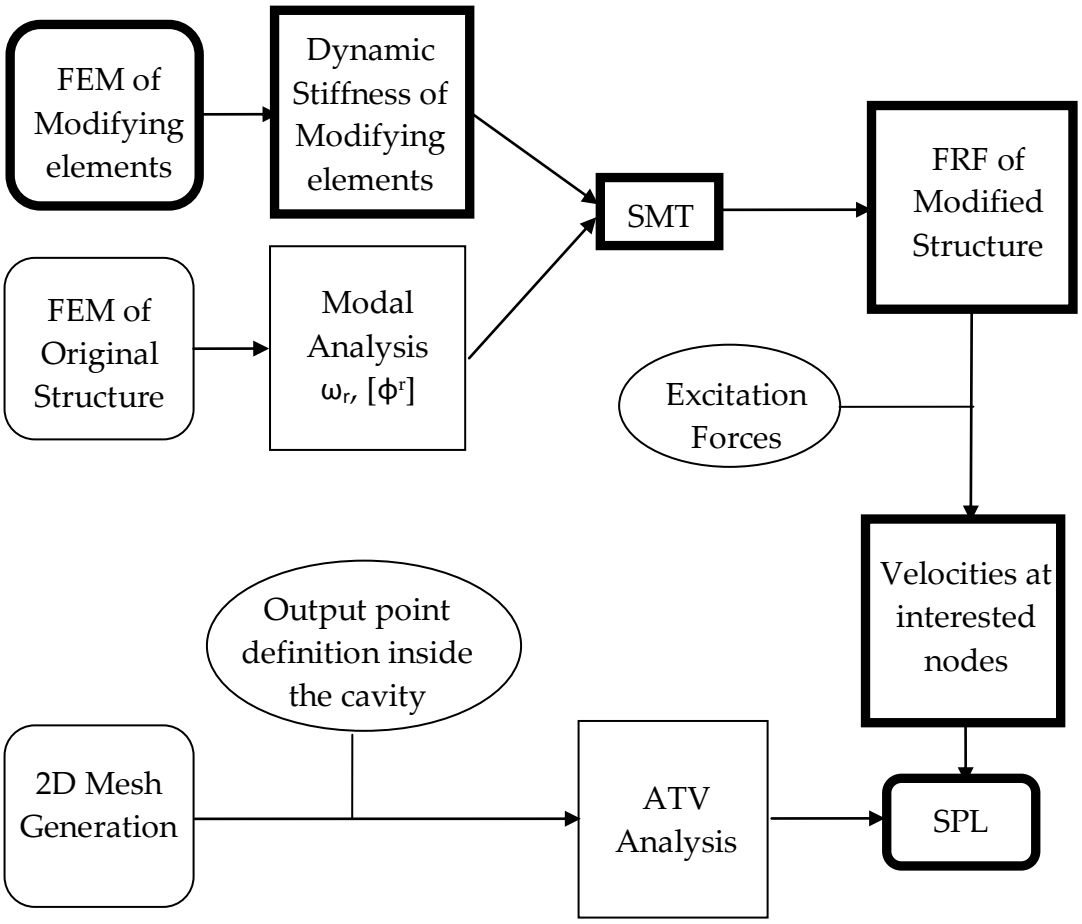

Figure 5.6 Flowchart explaining the FEM/BEM method with SMT

In the FEM/BEM method with SMT, modal analysis of the original model and ATV analysis are the most time consuming processes; but they are performed only once. Then, the steps marked with thick lines are repeated after changing the modification parameters.

Rectangular structure with fine mesh explained in the previous case studies is further investigated for acoustic analysis using BEM in the following case studies.

5.5.1 Case Study 9 – Direct FEM/BEM Method vs. FEM/BEM Method with SMT

Acoustic pressure at the output point is obtained with standard FEM/BEM method and compared with the FEM/BEM method used with SMT for the unmodified structure. Modal analysis of the original structure is performed in ANSYS software. In both of the methods 0.01 structural damping is assumed. In the standard FEM/BEM method, finite element model and modal analysis results are imported to LMS Virtual Lab. Excitation force is defined within the LMS Virtual Lab and sound pressure is calculated with the use of ATVs. In the FEM/BEM method with SMT, FRFs of the original structure are obtained in MATLAB code and velocities at the mid-panel are found by multiplying the mobility with the excitation forces. The only flexible part of the original structure is the mid panel, so vibration velocities are defined only on the nodes of the mid panel for FEM/BEM method with SMT application case. These calculated vibration velocities are then imported into LMS Virtual Lab. Sound pressure at the output point is again calculated with the use of ATVs. In each case ATVs are calculated between 1-200 Hz

with 1 Hz increment. Harmonic excitation force is applied on the node at the middle of the mid panel. The applied force has unit amplitude.

The two dimensional boundary element mesh and output point are illustrated in Figure 5.7. The boundary element model details are given in Table 5.10. A-weighted sound pressure levels are obtained at the output point located at (444.4, 870.6, 746.4) mm on the spherical field mesh.

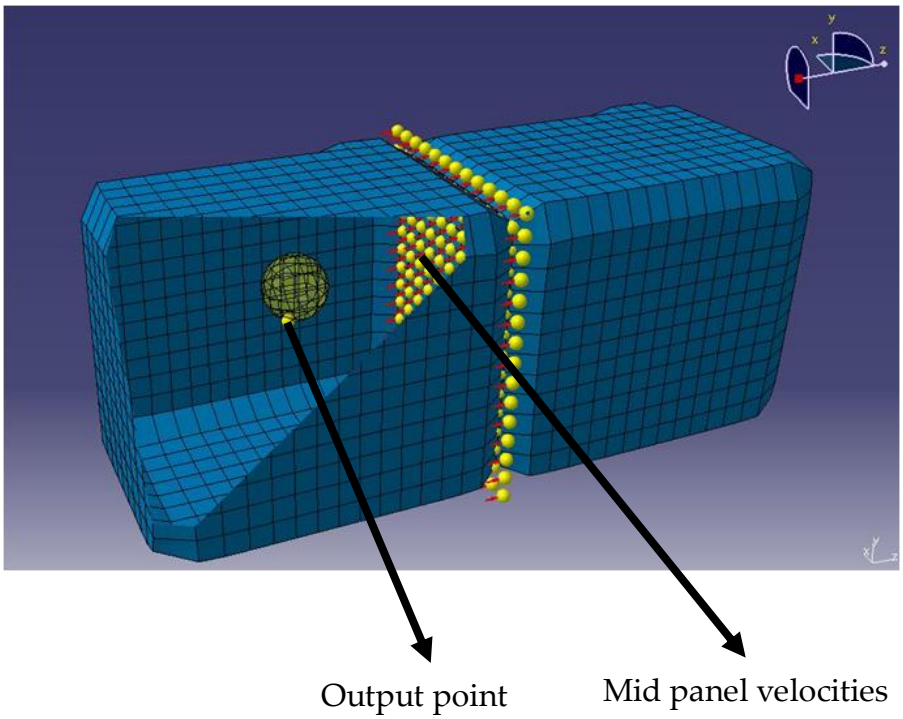

Figure 5.7 2D mesh of acoustic cavity

Table 5.10 Air properties and BEM details

Density ρ_0 [kg/m³]	1.225
Speed of sound c [m/s]	340
Number of elements (2D)	1800
Number of nodes	1804
Element edge length [mm]	100
Max frequency [Hz]	566.667

In order to validate the FEM/BEM method with SMT, the sound pressure at the output point is obtained with two methods and compared in Figure 5.8. The slight differences between two results are attributed to the difference between the two models: In standard FEM/BEM method vibration of all panels are taken into account, whereas in the FEM/BEM method with SMT vibration of only mid panel is considered. This difference does not cause a significant difference since the outer panels are almost rigid.

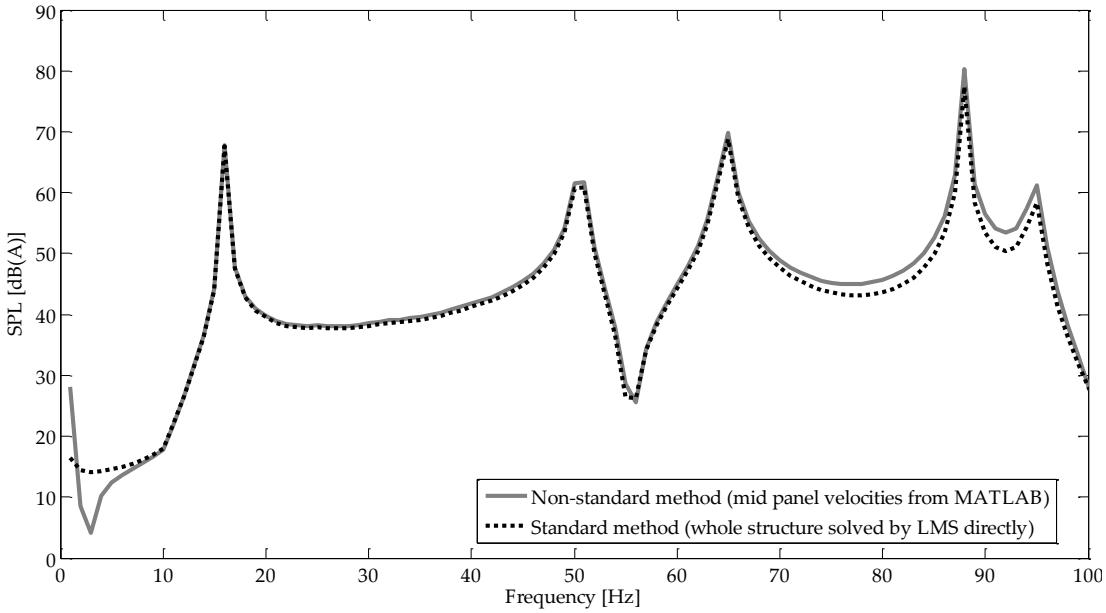

Figure 5.8 SPL (A) comparison for standard FEM/BEM method vs. FEM/BEM method with SMT

5.5.2 Case Study 10 – Effect of Stiffeners

In this part, the effects of changes in the width and location of the stiffeners on sound pressure level are investigated. The dimensions and properties of the original structure are given in Table 5.1 and finite element model details of the structure are given in Table 5.11. In the FRF and dynamic stiffness calculations, 0.01 structural damping is assumed. ATV analysis is performed for frequencies between 1-200 Hz with 1 Hz increment. The calculated transfer vectors are then used in each case.

Table 5.11 FEM details of the original structure

	Rectangular Box (without Mid-Panel)	**Mid-Panel**
Element type	Shell63	Shell63
Number of elements	856	168
Number of nodes	858	195
Degrees of freedom	5148	1170

Different configurations and different widths of steel strips are applied on the mid panel. The common properties and dimensions of stiffeners used in different cases are given in Table 5.12. The sound pressure at the output point is calculated after every modification step using FEM/BEM method with structural modification technique. The variable properties and locations are summarized in Table 5.13 for each case. The structural modification code is used in order to find modified structure's FRFs and velocities at the mid panel nodes. Unit amplitude excitation force is applied at the middle of the mid panel in the perpendicular direction to the surface and defined over the frequency range of interest. Imaginary and real components of calculated velocities are then exported to EXCEL files.

Table 5.12 Material properties and dimensions of stiffeners

	Modifying Strip
Modulus of elasticity E [GPa]	200
Density ρ_S [kg/m³]	7850
Poisson's ratio ν	0.3
Thickness [mm]	5
Length [mm]	1400

Table 5.13 Geometric and FEM details of stiffeners

Cases	**Width [mm]**	**# of strips**	**Location x [mm]**		**Element type**	**# of elements**	**# of nodes**	**# of dof**
A	30	1	600		Beam4	14	15	90
A200	30	1	800		Beam4	14	15	90
A400	30	1	1000		Beam4	14	15	90
B	40	1	600		Beam4	14	15	90
B200	40	1	800		Beam4	14	15	90
B400	40	1	1000		Beam4	14	15	90
C	30	2	200	1000	Beam4	28	30	180
D	30	2	400	800	Beam4	28	30	180
E	30	2	200	800	Beam4	28	30	180
F	50	1	600		Beam4	14	15	90
G	20	1	600		Beam4	14	15	90

Mid panel before any modification is illustrated in Figure 5.9. 1400 mm steels strips of different widths and locations are applied on the mid panel. Cases

presented in Table 5.13 are illustrated in Figure 5.10, Figure 5.11, Figure 5.12 and Figure 5.13.

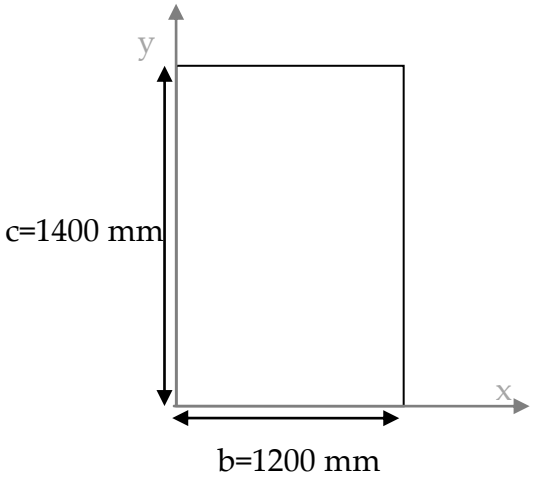

Figure 5.9 Mid panel before modification

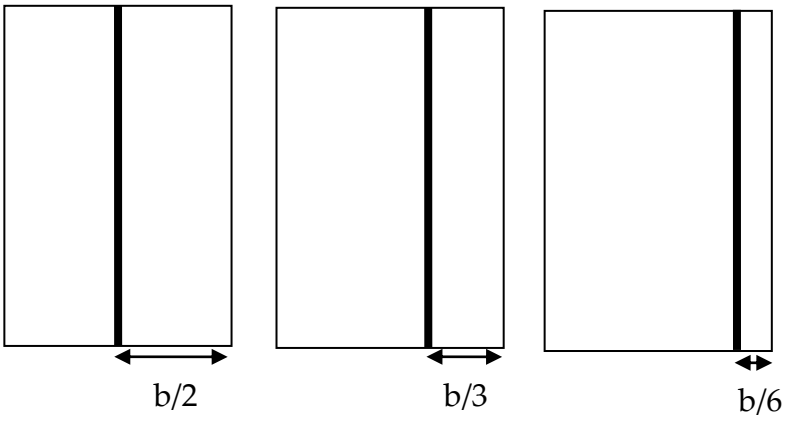

Figure 5.10 Case A; Case A200; Case A400 with 5x30 mm stiffener

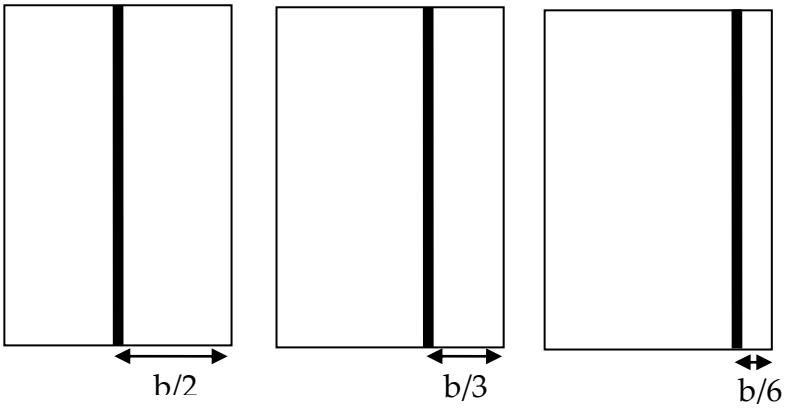

Figure 5.11 Case B; Case B200; Case B400 with 5x40 mm stiffener

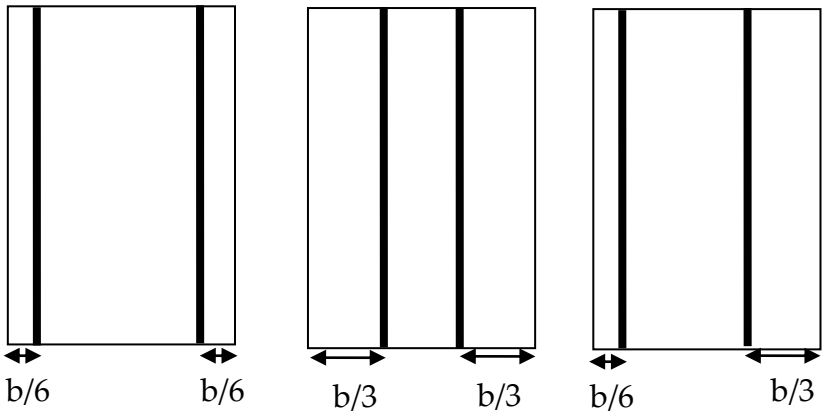

Figure 5.12 Case C; Case D; Case E with 5x30mm stiffener

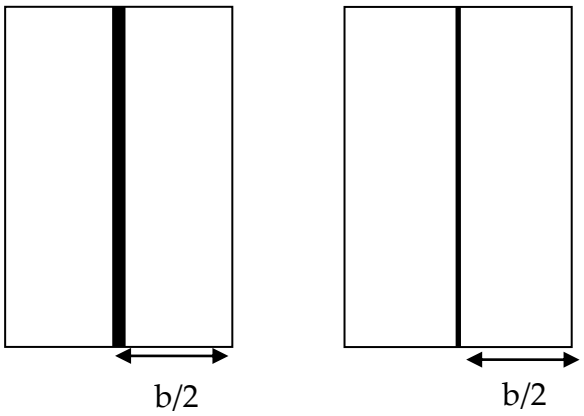

Figure 5.13 Case F with 5x50mm; Case G with 5x20mm stiffener

5.5.2.1 Effects of Position

The effects of stiffener location on the mid panel can be investigated by comparing sound pressures obtained at cases A, A200, A400, B, B200, B400, C, D and E. A-weighted sound pressures are obtained between 1-200 Hz with 1 Hz increment.

When Figure 5.14 is investigated, it is observed that stiffener application may increase the sound pressure levels at high frequencies. At low frequencies there is a frequency shift and at some frequencies, modifications do not lead to any change. The most effective location for this case is the mid of the panel. The similar comments can be made for Figure 5.15.

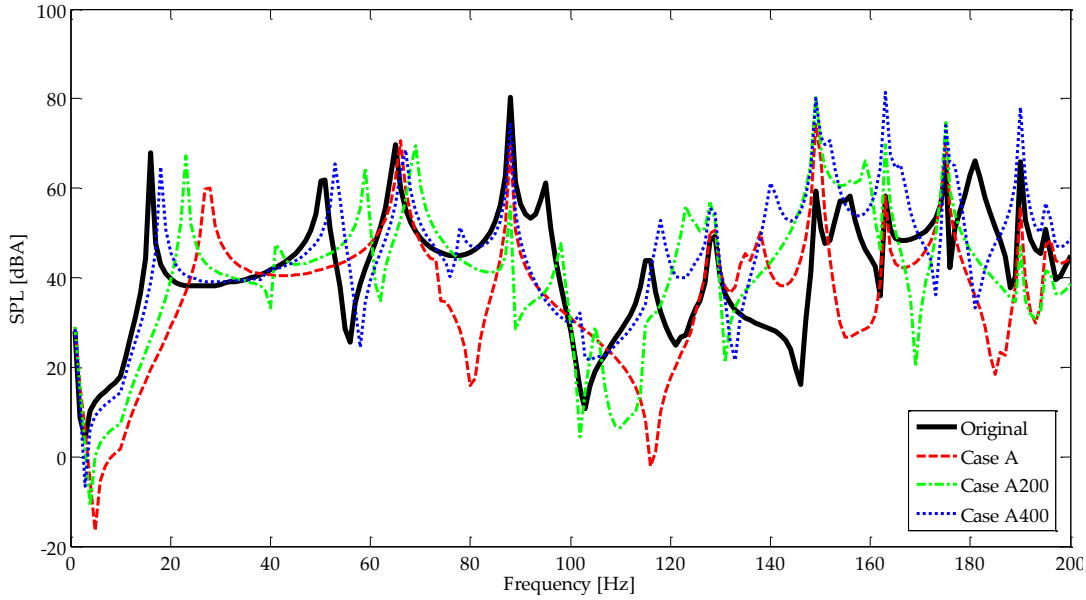

Figure 5.14 SPL (A) comparison cases A, A200 and A400

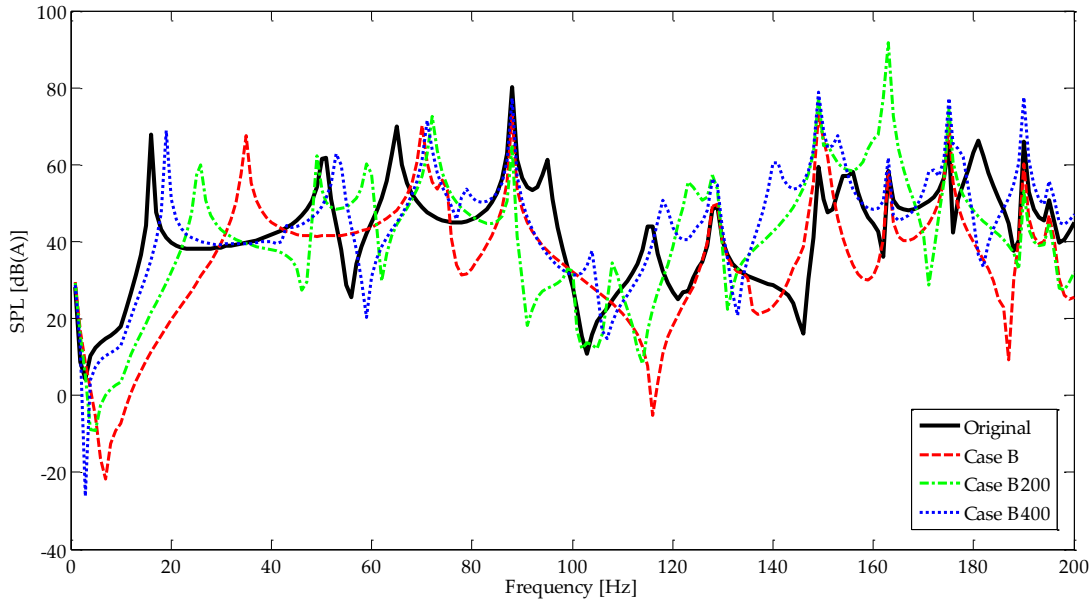

Figure 5.15 SPL (A) comparison cases B, B200 and B400

When two stiffeners are applied at different locations, the sound pressure results seem to increase especially at high frequencies as seen in Figure 5.16. Modifying the panel with two stiffeners does not seem to be effective in decreasing the acoustic pressure.

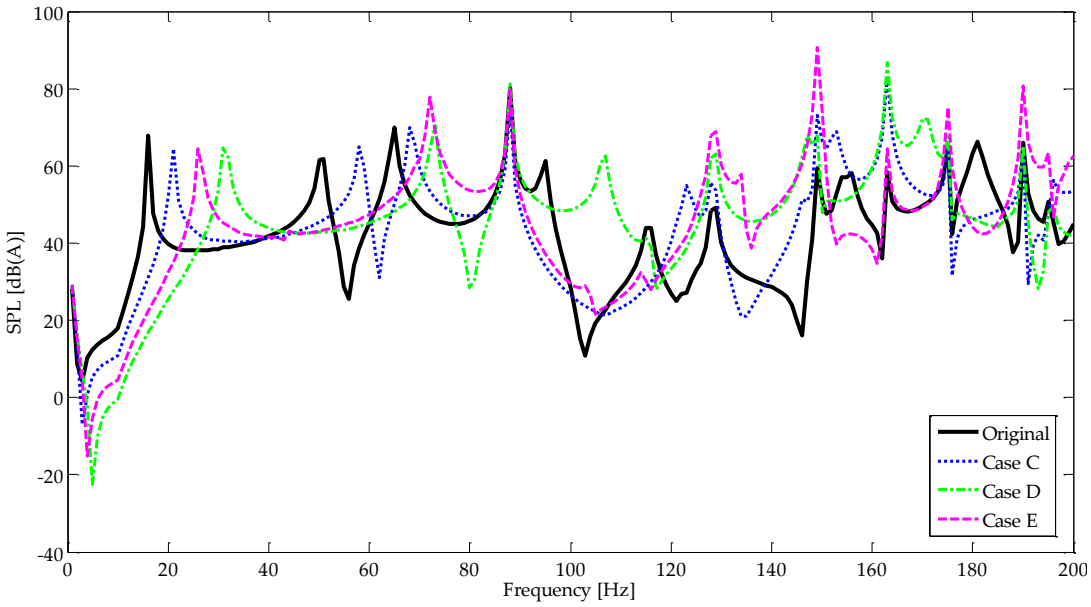

Figure 5.16 SPL (A) comparison cases C, D and E

5.5.2.2 Effects of Geometry

Modifications applied at the middle of the panel can be further investigated since they are the most effective ones among the cases studied. The effect of stiffener width can be studied by comparing cases G, A, B and F. The results are illustrated in Figure 5.17.

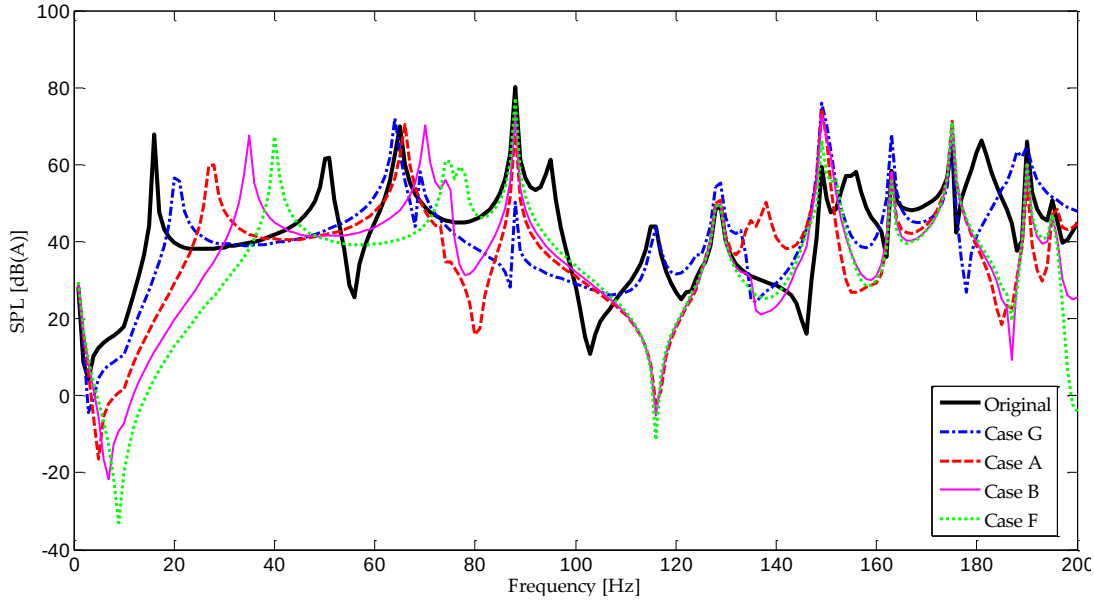

Figure 5.17 SPL (A) comparison cases G, A, B and F

As the modifying strip gets wider, there is a frequency shift to the right for the first peak. The narrowest strip, Case G, gives better results for some frequencies; particularly it decreases the SPL at 88Hz. However, for frequencies greater than 100 Hz, the widest strip, Case F, is more efficient to decrease the sound pressure levels.

Modifications applied in this chapter caused the peaks at 51 Hz and 155 Hz to diminish. The first peak at 18 Hz did not decrease significantly in all of the cases studied, but it is shifted to the right. Also, peak at 181 Hz disappeared in every presented case. The peak at 88 Hz was not affected from the modifications except for Case G.

CHAPTER 6

CONCLUSIONS

In this study effects of structural modifications on vibro-acoustic behavior of closed structures with vibrating boundaries are investigated. In popular classical approach, acoustic analysis procedure can be performed through a commercial software like LMS Virtual Lab, by implementing ATV method. Once the ATVs are calculated for a model, acoustic response due to vibrating surfaces is obtained very fast by only a matrix multiplication. However, the modal analysis of the vibrating structure has to be repeated after each modification on the structure. This requires considerable computational time, especially when the optimization of modification location, or modifications of elements are considered. This study employs structural modification technique integrated with the vibro-acoustic model of the system, and a practical approach is suggested exploiting the benefits of the structural modification technique. Then, results obtained by the proposed method are validated by comparing them with the ones obtained following the standard FEM/BEM analysis procedure. It is demonstrated that with this approach, modification results can be obtained in a fast and efficient way. The structural modification technique presented in this study proves itself to be very efficient for the case studies considered in this study to predict the sound pressure levels within vibro-acoustic systems.

6.1 Numerical Methods

The FEM/BEM combined method is used for the vibro-acoustic analysis. The structure is modeled with finite elements and modal analysis is performed. Different element types present in commercial FE software namely, CQUADR in NASTRAN/PATRAN library and Shell63 in ANSYS library, are used to model the structures and the results are compared with each other. It is observed that when Shell63 elements are used to model a free-free square plate, the natural frequencies are closer to the analytical results.

In the modeling effort of the closed rectangular cavity, either with shell elements or with solid elements, it is observed that there is a difference in the frequency response functions in higher frequency ranges. Upon consideration of applications on vehicle like structures, the analyses in the case studies are conducted using shell elements. Then, the effect of mesh size on the modal analysis is studied and an appropriate mesh size is selected.

The acoustic domain is modeled with boundary elements and it is mainly excited by the enclosing surfaces of the structure in vibration. In the BEM part, ATV method is used since the modifications do not change the geometry and acoustic properties of the acoustic cavity. Also, the effect of monopole as an acoustic source is investigated.

6.2 Structural Modification Technique

Structural modification technique which utilizes receptances of the original structure and the dynamic stiffness of added elements predicts the response

of the modified system without reanalyzing the whole system again. Matrix inversion is required in the method; however, the order of the matrix to be inverted is equal to the degrees of freedom of the modified region only. The modification method employed allows modifications causing an increase in the total degree of freedom of the system. Moreover, to decrease the matrix sizes, only the selected degrees of freedom of the original structure can be considered in the calculations. However, the degrees of freedom at connection points should always be retained. Elimination of redundant degrees of freedom does not cause error in the results.

For the structural modification with additional degrees of freedom, the results are obtained using the code prepared in MATLAB and validated by reanalysis of the modified structure using the finite element software. The effect of truncation is investigated and it is seen that truncation of modes affects the results at higher frequencies. The results obtained for lower frequencies are not affected from truncation.

The method is applied to different element types in NASTRAN/PATRAN and ANSYS libraries. It is observed that structural modification gives poor results when CQUADR elements are used to model the structure. In other words, the receptances of modified structure obtained by directly analyzing it in NASTRAN and those found by SMT are not perfectly matching, although no truncation is applied. This can be attributed to the reduction of degrees of freedom in mass matrices in NASTRAN/PATRAN. Structural modification technique gives good results for CBEAM elements in NASTRAN/PATRAN library; Shell63 and Beam4 elements in ANSYS library.

Therefore, the thin panels in the case studies are modeled with Shell63 elements, and Beam4 elements are preferred to represent the stiffeners.

The closed rectangular cavity is modified with stiffeners and the resulting sound pressure levels are presented for the cases with monopole and without monopole. The effect of structural modification is observed as different according to the acoustic source present in the domain. Without a monopole in the cavity, modified structure causes higher sound levels at some frequencies: For instance at 100-150 Hz and 190-200 Hz ranges and modification seems ineffective. However, the analysis performed involving a monopole shows that modification on the structure decreases sound levels at the predefined location at these frequencies.

6.3 Effect of Modifications on Sound Pressure Level

The approach proposed in this study (FEM/BEM method used with SMT) is applied to a rectangular structure having the sizes of a truck. Large panels of trucks vibrate and booming noise is a problem inside trucks [17, 34]. The properties and panel thicknesses are adjusted such that the natural frequencies are not too low and modal density at low frequencies is not very high.

The starting point of this study was to decrease low frequency noise (booming noise) inside vehicles by adding stiffeners to the panels. High frequency noise is not in the scope of this study since damping treatment is preferred to attenuate noise at high frequencies. Due to this reason, the analyses are performed between 0-200 Hz frequency range and structural

modifications by adding stiffeners are investigated to attenuate booming noise inside the closed structure.

Various finite element types and sizes were used in the analysis, and the results were compared from the accuracy point of view. Then, by using the approach suggested, different configurations of stiffeners with varying widths were applied to the mid-panel and the effects of stiffeners on the SPL at a specified point were studied.

From the results of the case studies it is observed that, stiffener addition is effective to decrease acoustic pressure at 0-200 Hz frequency range if applied in the middle of the panel. Then, width of the stiffener applied in the middle is varied. As the strip gets wider, first natural frequency shifts to higher frequencies due to stiffening effect. For the rest of the frequencies, wider stiffener is observed to be more effective to attenuate sound levels. However, the narrowest strip is also effective, especially in the 80-100 Hz range. An optimum stiffener width can be selected by comparing the results.

In the design stage of such a structure, an optimum modification can be determined by trying different parameters and comparing the results with some metrics such as loudness and sharpness. Using the proposed method, the effects of stiffener parameters on sound pressure levels are obtained in a fast and easy way.

6.4 Recommendations for Future Work

The FEM/BEM method with SMT can be improved by implementing an optimization routine. Data transfer between MATLAB and LMS Virtual Lab can be made simpler in order to make a serial data transfer.

The studied model is a very simple structure to represent a real vehicle. Furthermore, the contribution from only one panel is studied. The study can be extended by considering the other panels. Different excitations and effect of structural modifications to their responses can be investigated.

The cases where the stiffeners were placed near the edges resulted in higher amplitudes of sound pressure. Below coincidence frequencies, the radiation efficiency is affected significantly from the change in boundary conditions. In the case studies, the coincidence frequencies of the panels are much higher than the investigated frequencies so applying the stiffeners near the edges change the boundary conditions and radiation efficiency of the panel. So, for these cases, applying stiffeners may increase the acoustic pressure inside the cavity. This effect can be further investigated.

In the design and optimization stage, other parameters rather than the location and width can be considered. The most appropriate combination of parameters can be selected by careful and detailed numerical experimentation. FEM/BEM method combined with SMT allows testing more combination of parameters and this method can be further developed depending on the targeted application.

REFERENCES

[1] Özgüven H. N., *Structural Modifications Using Frequency Response Functions.* Mechanical Systems and Signal Processing, 1990, **4**: pp. 53-63.

[2] Lalor N., Priebsch H-H., *The prediction of Low- and Mid-Frequency Internal Road Vehicle Noise: a Literature Survey.* Proceedings of IMechE, Part D: J. Automobile Engineering, 2007, **221**: pp. 245-269.

[3] Kim S. H., Lee J. M., Sung M. H., *Structural-Acoustic Modal Coupling Analysis and Application to Noise Reduction in a Vehicle Passenger Compartment.* Journal of Sound and Vibration, 1999, **225(5)**: pp. 989-999.

[4] Ning F., Liu G., Wei J., *Study on Calculating Acoustic Sensitivity of Car Cab Based on Finite Element Method*, in *International Congress on Sound and Vibration, ICSV14*, 2007, Cairns-Australia.

[5] Davidson P., *Structure-Acoustic Analysis; Finite Element Modeling and Reduction Methods*, Ph.D Thesis, Structural Mechanics, 2004, Lund University

[6] Sonearko B., *Interior Noise Modeling Using BEM.* First Workshop on Vehicle Noise Visualization and Identification.

[7] Liu Z. S., Lu C., Wang Y.Y., Lee H.P., Koh Y.K, Lee K. S., *Prediction of Noise Inside Tracked Vehicles.* Applied Acoustics, 2006, **67**: pp. 74–91.

[8] Vlahopoulos N., Allen M.J., *Integration of Finite Element and Boundary Element Methods for Calculating the Radiated Sound from a Randomly Excited Structure.* Computers and Structures, 2000, **77**: pp. 155-169.

[9] Coyette J. P., *The Use of Finite-Element and Boundary-Element Models for Predicting the Vibro-Acoustic Behaviour of Layered Structures.* Advances in Engineering Software, 1999, **30**: pp. 133-139.

[10] Deng Z., Cao Y., *Prediction and Noise Reduction Design of Car Interior Vibration and Noise*, in *Proceedings of International Congress and Exposition on Noise Control Engineering, 37th Inter-Noise*, 2008, Shanghai-China.

[11] İrfanoğlu B., *Boundary Element-Finite Element Acoustic Analysis of Coupled Domains*, Ph.D. Thesis, Mechanical Engineering Department, 2004, METU

[12] Kopuz Ş., Ünlüsoy Y. S. and Çalışkan M., *Boundary Element Method in the Development of Vehicle Body Structures for Better Interior Acoustics.* Boundary Element Technology VIII, 1993: pp. 46-55.

[13] Kopuz Ş., *An integrated FEM/BEM Approach to the Prediction of Interior Noise Levels of Vehicle Body Structures*, Ph.D. Thesis, Mechanical Engineering Department, 1995, METU

[14] Kopuz Ş., Ünlüsoy Y. S. and Çalışkan M., *Formulation of the Interior Acoustic Fields for Passenger Vehicle Compartments*, in *Proceedings of the Second International Congress on Recent Developments in Air and Structure Borne Sound and Vibration*, 1992.

[15] Kopuz Ş., Ünlüsoy Y. S. and Çalışkan M, *Examination of the Interior Acoustic Field in the Presence of Sound Leakage Through Openings.* Boudary Element Communications Journal, 1993, **5**(4): pp. 168-170.

[16] Citarella R., Federico L.,Cicatiello A., *Modal Acoustic Transfer Vector Approach in a FEM–BEM Vibro-Acoustic Analysis.* Engineering Analysis with Boundary Elements, 2007, **31**: pp. 248–258.

[17] Kamçı G., Başdoğan İ., Koyuncu A., Yılmaz İ., *Vibro-Acoustic Modeling of a Commercial Vehicle to Reduce the Interior Noise Level*, in *37th International Congress and Exposition on Noise Control Engineering, Inter-Noise*, 2008, Shanghai-China.

[18] Pluymers B., Desmet W., Vandepitte D., Sas P., *On the Use of a Wave Based Prediction Technique for Steady-State Structural-Acoustic Radiation Analysis.* Journal of Computer Modeling in Engineering & Sciences 2005, **7(2)**: pp. 173-184.

[19] Hepberger A., Priebsch H.-H., Desmet W., van Hal B., Pluymers B., Sas P., *Application of the Wave Based Method for the Steady-state Acoustic Response Prediction of a Car Cavity in the Mid-frequency Range*, in *Proceedings of ISMA*, 2002.

[20] Pluymers B., Desmet W.,Vandepitte D., Sas P., *Application of the Wave Based Prediction Technique for the Analysis of the Coupled Vibro-Acoustic Behaviour of a 3D Cavity*, in *Proceedings of ISMA*, 2002.

[21] B. van Hal, Vanmaele C., Desmet W., Silar P., Priebsch H-H. *Hybrid Finite Element – Wave Based Method for Steady-State Acoustic Analysis*, in *Proceedings of ISMA* 2004.

[22] Desmet W., *A Wave Based Prediction Technique for Coupled Vibro-Acoustic Analysis*, Division PMA, 1998, KULeuven

[23] B. Van Genechten, Pluymers B., Vanmaele C., Vandepitte D., Desmet W., *On the Coupling of Wave Based Models with Modally Reduced Finite Element Models for Structural-Acoustic Analysis*, in *Proceedings of International Conference on Noise and Vibration Engineering, ISMA*, 2006.

[24] Charpentier A., Prasanth S., Fukui K., *Efficient Model of Structure-Borne Noise in a Fully Trimmed Vehicle from 200Hz to 1kHz*, in *Proceedings of Inter-Noise, 37th International Congress and Exposition on Noise Control Engineering*, 2008, Shanghai-China.

[25] Cotoni V. Shorter P.J., Charpentier A., Gardner B., *Efficient models of the acoustic radiation and transmission properties of complex trimmed structures*, in *Proceedings of Inter-Noise*, 2005, Rio de Janeiro, Brazil

[26] Pavic G., *Noise Sources and Virtual Noise Synthesis*, in *Proceedings of Inter-Noise, 37th International Congress and Exposition on Noise Control Engineering*, 2008, Shanghai-China.

[27] Ramsey K. A., Firmin A., *Experimental Modal Analysis, Structural Modifications and FEM Analysis*, in *Proceedings of International Modal Analysis Conference, IMAC*, 1982.

[28] Guimaraes G. P., Medeiros E. B., *Using Transfer Path Analysis to Improve Automotive Acoustic Comfort*, in *Proceedings of Inter-Noise*, 2007, Istanbul-Turkey.

[29] Crowley J. R., Rocklin G. T., Klosterman A. L., Vold H., *Direct Structural Modification Using Frequency Response Functions*, in *Proceedings of International Modal Analysis Conference, 2nd IMAC*, 1984.

[30] Özgüven H. N., *A New Method for Harmonic Response of Non-Proportionally Damped Structures Using Undamped Modal Data.* Journal of Sound and Vibration, 1987, **117 (2)**: pp. 313-328.

[31] Köksal S., Cömert M. D., Özgüven H. N., *Reanalysis of Dynamic Structures Using Successive Matrix Inversion Method* in *Proceedings of the International Modal Analysis Conference, 24th IMAC*, 2006, St. Louis-Missouri.

[32] Köksal S., Cömert M.D., Özgüven H. N., *Comparison and Application of Reanalysis Methods*, in *Proceedings of International Modal Analysis Conference, IMAC*, 2007.

[33] Alan S., Budak, E. ve Özgüven, H. N., *Analytical Prediction of Part Dynamics for Machining Stability Analysis.* International Journal of Automation Technology, 2010, **4**(special issue on Modeling and Simulation of Cutting Process).

[34] Başdoğan İ., Canbaloğlu G., Kamçı G., Özgüven H. N., *A Structural Modification Methodology Adapted To a Vibro-Acoustic Model to Improve the Interior Noise*, in *Euronoise,* , 2009, Edinburgh-UK.

[35] Canbaloğlu G., Özgüven H. N., *Structural Modifications with additional DOFApplications to Real Structures*, in *Proceedings of International Modal Analysis Conference, 27th IMAC* 2009, Orlando-USA.

[36] Çalışkan M., *ME 432 Acoustics and Noise Control Enginering Course Lecture Notes,* Mechanical Engineering Department, Middle East Technical University.

[37] Dhandole S. D., Modak S. V., *Review of Vibro-Acoustics Analysis Procedures for Prediction of Low Frequency Noise Inside a Cavity*, in *Proceedings of International Modal Analysis Conference, 25th IMAC*, 2007, Orlando-USA.

[38] Carlsson H., *Finite Element Analysis of Structure-Acoustic Systems; Formulations and Solution Strategies*. cited in "Davidson P., *Structure-Acoustic Analysis; Finite Element Modeling and Reduction Methods*, Ph.D Thesis, Structural Mechanics, 2004, Lund University", 1992.

[39] Ali A., Rajakumar C., *The Boundary Element Method Applications in Sound and Vibration*, 2004: A.A. Balkema Publishers.

[40] Chen Z., Hofstetter G., Mang H., *A Galerkin–type BE–formulation for Acoustic Radiation and Scattering of Structures with Arbitrary Shape*, in *Computational Acoustics of Noise Propagation in Fluids – Finite and Boundary Element Methods*, Marburg S., Nolte B., Editor, 2008, Springer, pp. 435-458.

[41] *LMS SYSNOISE Manual Rev 5.5*, in *Modeling Principles*.

[42] F. Fahy J., *Statistical energy analysis: a critical overview*, in *Statistical Energy Analysis; An Overview, with Applications in Structural Dynamics*, Keane A. J., Price W. G., Editor, 1997, Cambridge University Press, pp. 1-18.

[43] Ramirez H. I., *Multilevel Multi-Integration Algorithm for Acoustics*, Ph.D. Thesis, 2005, University of Twente

[44] Ottosen N., Peterson H, *Introduction to the Finite Element Method*. cited in "Davidson P.,*Structure-Acoustic Analysis; Finite Element Modeling and Reduction Methods*, in *Structural Mechanics*. 2004, Lund University", 1992, New York: Prentice Hall.

[45] Guyan R.J., *Reduction of Stiffness and Mass Matrices.* AIAA Journal, 1965, **3 (2)**: pp. 380.

[46] Blevins R. D., *Formulas for Natural Frequency and Mode Shape*, 1979, Malabar, Florida: Krieger Publishing Company.

[47] Marburg S., *Discretization Requirements: How many Elements per Wavelength are Necessary?*, in *Computational Acoustics of Noise Propagation in Fluids - Finite and Boundary Element Methods*, N.B. Marburg S., Editor, 2008, Springer: Berlin Heidelberg.

[48] Leissa A. W., *Vibration of Plates*. Ohio State University, 1969, Washington, D.C.: US. Government Printing Office.

[49] Vigran T. E., *Building Acoustics*. 2008, Taylor & Francis: Abingdon.